

IMPACTS OF URBAN GROWTH UPON AQUIFER RECHARGE:
A CASE STUDY OF THE BARTON SPRINGS ZONE OF
THE EDWARDS AQUIFER

by

Nathaniel K. Pasley, B.S.

A thesis submitted to the Graduate Council of
Texas State University in partial fulfillment
of the requirements for the degree of
Master of Science
with a Major in Geography
December 2022

Committee Members:

T. Edwin Chow, Chair

Benjamin Schwartz

Nathan Currit

COPYRIGHT

by

Nathaniel K. Pasley

2022

FAIR USE AND AUTHOR'S PERMISSION STATEMENT

Fair Use

This work is protected by the Copyright Laws of the United States (Public Law 94-553, section 107). Consistent with fair use as defined in the Copyright Laws, brief quotations from this material are allowed with proper acknowledgement. Use of this material for financial gain without the author's express written permission is not allowed.

Duplication Permission

As the copyright holder of this work I, Nathaniel Pasley, authorize duplication of this work, in whole or in part, for educational or scholarly purposes only.

DEDICATION

I dedicate this thesis to my children – Nathan and Zachary. You are both guiding lights in my life, and I am grateful and honored to be your father. I implore you to strive every single day of your life to be your best self, to realize your dreams, to never let anyone tell you that you can't do something, and to live your life in a way that makes you proud of yourself. In your darkest moments, look inside and find the strength to continue confidently along your path.

To my mother – Catherine. Thank you for your sacrifice. Thank you for always believing in me, even when I didn't believe in myself, and thank you for your love. You have taught me what hard work brings, what joy dedication can offer, and what it means to be committed to a goal. Without the hardships we've been through, this would not have been possible, so I thank you for never giving up on me.

And to my best friend – Kyle. You are the brother I never had, and the friend I've always needed. You have taught me the meaning of true friendship, and how to love and tolerate others, as well as myself. Without your influence in my life, I would undoubtedly be a lesser man, and I will always be grateful for it. I hope I've been half the friend to you, that you have been to me. I finished, man... I finished.

ACKNOWLEDGEMENTS

I would like to thank my graduate advisor – Dr. T. Edwin Chow, for his invaluable mentorship throughout this journey. His tireless commitment to excellence has taught me so much more than geography, and I am forever grateful for his teaching. Without which, realizing this dream would not have been possible.

Additionally, I would like to thank my two committee members – Dr. Benjamin Schwartz, and Dr. Nate Currit. Their expertise and wisdom have brought me constant inspiration throughout my college education, and I endeavor to pursue a life of enlightenment as they have taught me.

Finally, I would like to thank the faculty and staff of the Texas State Geography Department. From the day I arrived here, I knew I was home. Your dedication to the student body, and to the discipline of geography, has solidified in me the confidence to follow my dreams, and to believe in myself as you believe in me. From the bottom of my heart, I thank you all.

TABLE OF CONTENTS

	Page
ACKNOWLEDGEMENTS.....	v
LIST OF TABLES.....	viii
LIST OF FIGURES.....	ix
LIST OF ABBREVIATIONS.....	xi
ABSTRACT.....	xiii
CHAPTER	
1.0 INTRODUCTION.....	1
1.1 Problem Statement.....	5
1.2 Objectives.....	6
1.3 Justification.....	6
2.0 LITERATURE REVIEW.....	8
2.1 Overview.....	8
2.2 Overview of the SLEUTH Urban Growth Model.....	10
2.3 Overview of Groundwater Modeling.....	15
2.4 Case Studies in Urban Policy, Growth, and Hydrology.....	19
2.5 Case Studies in Central Texas.....	21
3.0 MATERIALS AND METHODS.....	25
3.1 Study Area.....	25
3.2 Urban Growth Model Data and Pre-processing.....	27
3.2.1 Urban.....	27
3.2.2 Transportation (Roads).....	28
3.2.3 Exclusion.....	29
3.2.4 Slope.....	30
3.2.5 Hillshade.....	30
3.3 SLEUTH Model Calibration.....	30
3.4 Hydrologic Model Data and Pre-processing.....	32

3.4.1 Soil Group.....	32
3.4.2 LULC	33
3.4.3 Soil-Water Capacity.....	33
3.4.4 Surface Water Flow Direction	33
3.4.5 Climatological Data	34
3.4.6 Lookup Tables	34
3.5 SWB Model Calibration	34
3.6 Urban Growth and Recharge Scenarios.....	35
4.0 RESULTS	39
4.1 SLEUTH Model Calibration Results.....	39
4.2 SWB Model Calibration Results.....	39
4.3 SLEUTH Model Results.....	41
4.3.1 Current Land-Use.....	41
4.3.2 Baseline Scenario.....	43
4.3.3 Extreme Scenario	44
4.3.4 Conservative Scenario	45
4.3.5 Aggressive Scenario.....	46
4.4 SWB Model Results.....	47
4.4.1 Current Mean Annual Recharge	47
4.4.2 Baseline Scenario.....	49
4.4.3 Extreme Scenario	50
4.4.4 Conservative Scenario	51
4.4.5 Aggressive Scenario.....	52
4.5 Hypothesis Testing.....	53
5.0 DISCUSSION.....	56
5.1 SLEUTH Calibration	56
5.2 SWB Calibration.....	58
5.3 SLEUTH Scenarios.....	59
5.4 SWB Scenarios	63
5.5 Hypothesis Testing.....	66
5.6 Limitations	67
6.0 CONCLUSION.....	70
REFERENCES	72

LIST OF TABLES

Table	Page
1. Prescribed waterway classification criteria and stream buffer sizes as prescribed by the City of Austin – Environmental Criteria Manual (City of Austin, 2022b).....	30
2. Net Site Area calculation table taken from Appendix Q-1 of the City of Austin – Environmental Criteria Manual (City of Austin, 2022c).....	37
3. Results of the SLEUTH calibration routine showing the best fit coefficients used in the baseline, conservative, and aggressive scenarios (BFC), and the best fit coefficients used in the extreme scenario (BFC extreme).....	39
4. Results of the SWB calibration routine showing mean annual recharge values for stream gage sites used for calibration.....	40
5. Summary of area urbanized in the NLCD 2019 LULC data and area predicted to urbanize by SLEUTH through the year 2042 for each scenario.....	42
6. Summary of the percent change in area urbanized between each SLEUTH scenario output and the NLCD 2019 LULC data.....	43
7. Summary of current mean annual recharge based on NLCD 2019 LULC data, and mean annual recharge based on SLEUTH scenarios as modeled by SWB.....	49
8. Summary of the percent change in mean annual recharge between each SWB scenario output and the current mean annual recharge based on NLCD 2019 LULC data.....	49

LIST OF FIGURES

Figure	Page
1. The recharge and contributing zones of Barton Springs.....	4
2. Landsat 8 imagery of the study area	28
3. USGS stream gages used for calibration of the SWB model.....	40
4. NLCD LULC 2019 data for the study area.....	42
5. Urbanization as of 2042 as predicted by SLEUTH, urbanization as of 2019 in the NLCD 2019 LULC data, and the 2020 roads input layer for the baseline scenario	44
6. Urbanization as of 2042 as predicted by SLEUTH, urbanization as of 2019 in the NLCD 2019 LULC data, and the 2020 roads input layer for the extreme scenario	45
7. Urbanization as of 2042 as predicted by SLEUTH, urbanization as of 2019 in the NLCD 2019 LULC data, and the 2020 roads input layer for the conservative scenario	46
8. Urbanization as of 2042 as predicted by SLEUTH, urbanization as of 2019 in the NLCD 2019 LULC data, and the 2020 roads input layer for the aggressive scenario	47
9. Current mean annual recharge as modeled by SWB	48
10. Mean annual recharge for the baseline scenario as predicted by SWB	50
11. Mean annual recharge for the extreme scenario as predicted by SWB	51
12. Mean annual recharge for the conservative scenario as predicted by SWB	52
13. Mean annual recharge for the aggressive scenario as predicted by SWB	53
14. Scatterplot showing mean annual recharge as a function of area urbanized by SLEUTH for each zone in each scenario	54

15. Boxplots showing the range, minimum, maximum, and mean values of each zone as predicted by SWB for the baseline scenario55

LIST OF ABBREVIATIONS

Abbreviation	Description
CAPCOG	Capital Area Council of Governments
MSA	Metropolitan Statistical Area
LULC	Land-Use/Land-Cover
CZ	Contributing Zone
RZ	Recharge Zone
BSZ	Barton Springs Zone
SOS	Save our Springs
COA	City of Austin
SWB	Soil-Water Balance
GEAA	Greater Edwards Aquifer Authority
CA	Cellular Automata
OSM	Optimal SLEUTH Metric
ESP	Ecological Security Patterns
GIS	Geographic Information System
CLUE-S	Conversion of Land-Use and its Effects at Small regional extent
WetSpass	Water and Energy Transfer between Soil, Plants, and Atmosphere under quasi-Steady State
2CAFDYM	Cellular Automaton for Flow Dynamics Model

SWAT	Soil Water Assessment Tool
I-CAT	Impervious Change Analysis Tool
USGS	United States Geological Survey
WC	Williamson Creek
NDVI	Normalized Difference Vegetation Index
NLCD	National Land-Cover Database
UMT	Urban Morphology Types
MLC	Maximum Likelihood Classification
TxDOT	Texas Department of Transportation
CWQZ	Critical Water Quality Zone
WQTZ	Water Quality Transition Zone
NSA	Net Site Area
BFC	Best Fit Coefficients
MCI	Monte Carlo Iterations
NI	Number of Iterations

ABSTRACT

Over the last 30 years, Austin, TX has experienced extremely high population growth. As the city expands to accommodate new residents, the surrounding natural environment is at risk of degradation. The Edwards Aquifer is a karst aquifer system that supplies drinking water to nearly two million people throughout central Texas but is highly vulnerable to changes at the land surface. In 1992, the Save Our Springs Ordinance was passed to prevent degradation to water quality and quantity in the Edwards by limiting urban development in zones contributing to Barton Springs Pool in central Austin. This research applies a scenario-based Cellular Automata urban growth model coupled with a soil-water balance model to examine future urban growth patterns and the resulting impacts to aquifer recharge in the Barton Springs Zone of the Edwards Aquifer. It seeks to contribute sound scientific information regarding optimal limits to urban development that facilitate sustainable growth that can be used to guide future urban planning initiatives in Austin.

1.0 INTRODUCTION

Today, about 57% of the world's population lives in urban areas (Demographia, 2022), up from 29% in 1950, and 14% in 1900 (Wu et al., 2014), and this number is projected to increase to 70% by 2050, and 100% by 2092 (Batty, 2011). As of 2017, more than 80% of the U.S. population lived in urban areas despite only 3% of its land mass being classified as urban (U.S. Census Bureau, 2017), and the decade 2010 – 2020 was the first in U.S. history to see a decline in rural population (Johnson, 2022). The decline is attributed to an aging rural population and out-migration of rural youth in search of higher education (Clark et al., 2016), better health care and entertainment (Torrey, 2004), and more job opportunities as mechanization of agriculture, timber, and mining operations has dwindled rural economies (Smith et al., 2016).

From 1970 – 2010, the percentage of Texas residents living in urban centers grew by 5% (Iowa Community Indicators Program, 2022). During the same time, the state added almost 14 million people (Texas State Library, 2020), and 85% of them lived in urban areas (White et al., 2017). Most new residents come from other parts of Texas, followed by California, Florida, New York, and Illinois (Austin Chamber of Commerce, 2022a). Texas is home to the nation's second largest economy by gross domestic product, and it is also the tenth largest economy in the world (Texas Politics Project, 2022), making it an attractive place for those seeking opportunity and a stable income.

Over the last decade, the state capitol—Austin, has seen a rapid and robust influx of these new residents. The Capital Area Council of Governments' (CAPCOG) Comprehensive Economic Development Strategy (2021) declared the Austin-Round Rock-Georgetown Metropolitan Statistical Area (MSA) the fastest-growing large metro

area in the United States from 2010 – 2020. Hays and Williamson counties to the south and north of Austin, respectively, were the first- and third-ranked counties in Texas in terms of growth rate during the same period, and collectively, the region grew at a rate that nearly doubled the statewide average and more than four times the national average (CAPCOG, 2021). Austin ranked fourth in the U.S. for population growth from 2020 – 2021, adding 146 new residents a day (U. S. Census Bureau, 2022) and is projected to be the third most populous MSA in Texas by 2050, with a total population of over 5 million people (Hobby Center for Public Policy, 2014). Furthermore, Austin’s economy remained resilient throughout the COVID-19 pandemic, as it added almost 90,000 new jobs to pre-pandemic levels and is the second best performing major job market since the pandemic began in 2020 (Austin Chamber of Commerce, 2022b), thus placing Austin in a strong economic position to support a prolonged population boom.

Prosperity does not come without a price, however. Urbanization, or the conversion of agricultural or open space land-use to residential, commercial, industrial, or transportation has been linked to habitat fragmentation (Zhu et al., 2020), species loss in birds (Dri et al., 2021), disruption of ecosystem services (Wang et al., 2021a), increased air pollution (Shi et al., 2022), and CO² emissions (Yao et al., 2021). Moreover, there is ample evidence that land-use/land-cover (LULC) is inextricably connected to the quantity and quality of groundwater (Prabhakar and Tiwari, 2015; Yar, 2020; Zhang and Schilling, 2006). Moreover, impervious cover and deforestation have been shown to have significant impacts upon rainfall infiltration, runoff, evapotranspiration, and aquifer recharge (Liaqet et al., 2021; Mondal et al., 2020; Sonoda, et al., 2001). Therefore, as Austin experiences rapid population growth in the coming decades, there is a need for

environmentally sustainable urban growth management by planners and policymakers to ensure the stewardship of its natural resources for future generations.

The Edwards Aquifer is a karst limestone aquifer of Cretaceous age located in central Texas. It is one of the most prolific aquifers in the world and supplies more than 50% of drinking water to the cities of Austin and San Antonio (U. S. Geological Survey, 2021a), as well as the many suburbs and rural areas in between. Karst aquifers are highly susceptible to direct inputs of rainfall at the surface via solution features like sinkholes, caves, fissures, and structural features like geologic faults. Because these features increase opportunities for aquifer recharge, they also increase the vulnerability of groundwater to contamination (U. S. Geological Survey, 2021b). Below Austin lie portions of both the Edwards Aquifer *Contributing Zone* (CZ)—land characterized by allogenic recharge, where overland flow drains in the southeastern direction over thin soils, and impermeable outcrop to the extremely sensitive *Recharge Zone* (RZ)—land characterized by autogenic recharge with highly permeable karst features, where large amounts of surface runoff infiltrate and recharge the aquifer. Barton Springs, a popular artesian watering hole in central Austin and home to two federally-endangered species derives its pristine waters from the Edwards CZ and RZ through preferential subterranean flow paths running in a general north-northeast direction throughout the RZ. The Barton Springs Zone (BSZ) (Figure 1) is comprised of six watersheds that straddle portions of both the CZ and RZ, where dye tracing tests have shown travel times to the outlet at the Springs to be as fast as 2.4 days (Zappitello et al., 2019). Since the 1990's, nitrate concentrations have increased by 20% from urbanization and increased wastewater generation (Musgrove et al., 2016).

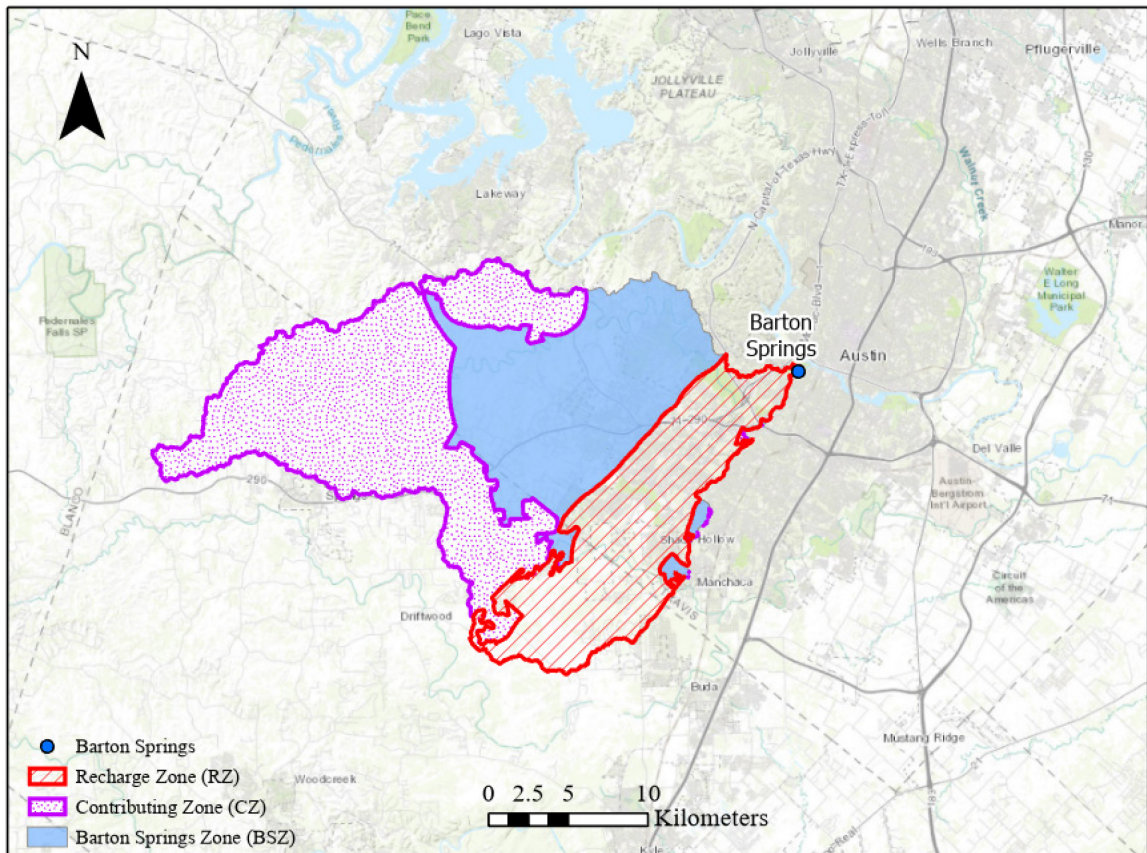


Figure 1. The recharge and contributing zones of Barton Springs.

In 1990, plans for a 4,000-acre development in the Barton watershed threatened to encroach upon Barton Springs Pool, and more importantly, the highly sensitive CZ and RZ of the BSZ. In response, a loose coalition of concerned citizens formed the Save Our Springs Alliance to help educate and inform the public about the proposed development and petitioned the Austin City Council to delay or deny construction. On June 7th, 1990, more than 800 citizens showed up to speak in opposition to the development at a night-long council meeting, after which, council members unanimously rejected the project and provided the momentum that would eventually lead to one of Austin’s most significant water quality protection initiatives. On August 8th, 1992, the Save Our Springs (SOS) Ordinance was approved by voters by an almost 2:1 ratio and included limits of 15 – 25%

impervious cover in sensitive zones, as well as more stringent regulations on levels of pollutants found in precipitation runoff. Despite the many lawsuits and appeals that followed (the Texas Supreme Court chose to uphold the ordinance in 1998), the ordinance is still intact today. Article 13 of Subchapter A, Chapter 30-5 in the City of Austin, Texas Code of Ordinances covers the SOS initiative. Section 30-5-514 declares that:

“In the watersheds contributing to Barton Springs... impervious cover shall be limited to a maximum of 15% in the entire recharge zone, 20% of the contributing zone within the Barton Creek watershed, and 25% in the remainder of the contributing zone.” (City of Austin, 2022a)

Impervious cover limitations established by the City of Austin (COA) are a function of a watershed’s relationship to the city’s drinking water supply, and the relative age of the development in question (Watershed Protection Department, 2016a). There are currently five watershed classifications established by the City that determine the level of land development regulations applied to new construction. Urban and Suburban watersheds combine to form the Desired Development Zone, which has the least amount of regulation, and Water Supply Suburban, Water Supply Rural, and the BSZ form the Drinking Water Protection Zone, which has the most regulation and is where SOS is enforced.

1.1 Problem Statement

Current urban growth rates in the Austin area show no signs of slowing, and projections show that Austin may one day exceed the capacity of the surrounding natural environment to support this growth. Considering the impact that impervious cover has been shown to have on both surface and groundwater processes, and the importance of SOS in protecting these processes for the preservation of Austin’s water supply,

stakeholders can benefit from an assessment of the impacts of impervious cover limits to amounts of aquifer recharge derived in the BSZ. The urban growth model is a tool used to forecast urban growth patterns, where its outputs can be used to model the corresponding aquifer recharge.

1.2 Objectives

This research will address two main objectives:

1. Simulate future urban development patterns in BSZ watersheds through the year 2042 under various scenarios of impervious cover limits, and
2. Investigate the impact of varying impervious cover on potential aquifer recharge through the year 2042.

1.3 Justification

The Greater Edwards Aquifer Alliance (GEAA), a non-profit organization that advocates for protection and preservation of the Edwards Aquifer (*Aquifer Alliance*, 2022), has suggested lowering the current SOS limits to impervious cover to 10% in the recharge zone, and 15% in the contributing zone (Greater Edwards Aquifer Alliance, 2021). Meanwhile, the median sales price of homes in the Barton Creek area between July 2021 – July 2022 was 1.96 million dollars (*Listings*, 2022). With plans for more construction (Bassman, 2019; Benavidez, 2021; Higgins, 2022; Novak, 2021), the BSZ is one of the most sought-after locations for Austin real-estate developers. The COA includes environmental sustainability as a factor when making policy decisions, and flood, erosion, and water quality impacts help prioritize funding for capital projects (Watershed Protection Department, 2016b). Therefore, knowing future alterations to impervious cover and subsequent BSZ hydrology is an important insight that

stakeholders can use to inform future decisions.

Urbanization has an undeniable impact on both surface and groundwater hydrology (Giardino & Houser, 2015; Guerra & Debagge, 2021; Sung et al., 2013), and impervious surface is a key indicator of urban watershed health (Brabec, 2009). Given that the SOS Ordinance is under pressure as developers seek to build in the BSZ, its effectiveness in protecting recharge and water quality in the Edwards Aquifer should be analyzed under future growth scenarios. Tracking future impervious cover expansion and patterns, as well as the hydrologic impacts they bring, is of importance to decision makers in Austin's urban development process and can help ensure that urban growth takes place sustainably regarding its impact upon aquifer recharge.

2.0 LITERATURE REVIEW

2.1 Overview

Predictive modeling is “the process of developing a mathematical tool or model that generates an accurate prediction” (Kuhn & Johnson, 2013). Today, these tools are all around us. The vast amount of information available on the internet has now given scientific researchers, as well as the layman, an almost infinite supply of data with which to build, test, and deploy such tools. Technology that was once reserved only for the most cutting-edge Sci-Fi novels is now an integral part of our daily lives. Predictive tools are embedded in, and provide core functionality to, devices such as the Google search bar, Global Positioning Systems, cell phones, automobiles, kitchen appliances, and even our thermostats. To many, the term predictive modeling is associated with machine learning techniques like knowledge discovery, pattern recognition, neural networks, or data mining. Although these methods are an appropriate association to make, as they most often form the methodological backbone to modeling tools, predictive modeling is also concerned with the underlying processes that lead to a digestible, reasonable, and highly trustable model output form (Kuhn & Johnson, 2013), a concept that is central to all geographic study.

A basic premise in geography is that in order to understand the spatial form of a phenomenon, one must reconstruct the latent antecedent process by which it was created (Norton, 1978). Geographers know this relationship as *process and form*. Process represents the underlying patterns, mechanisms, and relationships between geographic entities that manifest into higher dimensions of functionality. Form is the outward spatial distribution, arrangement, and shape that is limited by its governing processes. Forms

change with time, however, and because of the mutual interaction between process and form, one may infer much information about time and place of a given process based solely on its form, or vice-versa (Eichenbaum & Gale, 1971).

In urban planning, space is a key resource for meeting human need through urban design--“the process of giving form, shape, and character” to buildings, neighborhoods, and, eventually, entire cities (Raven et al., 2018). The highest priority to urban planners is to understand and shape the physical environment to help communities meet their purpose (Lynch & Rodwin, 1958), but meeting these needs involves processes that often manifest in unsustainable forms of urban design, thus creating harmful feedback loops between the built environment, the natural environment, and their respective inhabitants (Aminpour et al, 2022; Bao & He, 2019; Churkina, 2016; Fry, 2011; Miles et al., 2019). In other words, all actions taken by human societies inevitably reverberate throughout the natural world with varying degrees of consequence, and once their compounding effects reach given thresholds, certain degrees of consequence are reciprocated to humans by the natural world. This confluence of civil planning, design, implementation, and construction with natural resources, earth systems, and the biota they support provides a perfect opportunity for predictive models to offer valuable insights that can help harmonize future human development with the natural world.

Geographic information is a critical component for the accurate representation of both process and form, as well as the agents that drive them, in modern predictive models. Geocomputation is a useful tool that is well-suited for leveraging geographic data in conjunction with these mathematical tools. It is “the adoption of a large-scale computationally intensive scientific paradigm ... for doing all manner of geographical

research” (Openshaw et al., 2014). A geocomputational technique that is widely used for simulating the spread, or growth, of geographic phenomena is cellular automata (CA). Based on work by von Neumann & Burkes (1966), Wolfram (1994), Hagerstrand (1967), and Tobler (1979), CA simulates a system of interest by conceptualizing space and time as a grid of equal-sized cells, where each cell’s characteristics, or state, is one of a finite group of possible states predetermined by the modeler and is a function of the states of adjacent cells within a local neighborhood. Transition rules govern how adjacent cell states affect the cell being evaluated and are often implemented programmatically as ‘If-Then’ statements. CA models are keenly adept at simulating spatial morphologies as fractal patterns, and in this way, translate the local processes made up by individual agents to the global form they help create (Openshaw et al., 2014). This translative nature of CA lends itself well to the predictive modeling of urban growth, and in particular, one such model offers a well-developed tool to apply this technique.

2.2 Overview of the SLEUTH Urban Growth Model

SLEUTH is an acronym that lists the model’s input layers of Slope, Land-use, Exclusion, Urban, Transportation, and Hillshade. The San Francisco Bay area served as the pilot study area for SLEUTH modeling that forecast urban extents 100 years into the future (Clarke et al., 1996; Clarke et al., 1997; Clarke & Gaydos, 1998). Taking slope, land use, areas excluded from urbanization, existing urban extent, and hillshade as inputs, the SLEUTH model adopted a rigorous brute-force calibration routine and was shown to be capable of making sound predictions in many geographic areas (Ayazli, 2020; Bihanta et al., 2014; Chaudhuri & Clarke, 2019; Gómez et al., 2021; Guan & Rowe, 2016; Mekonnen & Ghosh, 2020; Rienow & Goetzke, 2015). Instead of deriving the outputs by general probability distributions, SLEUTH allows each cell to act

independently within the growth rules in a CA model. This study will use SLEUTH predictions of future urban extent to understand the efficacy of the SOS' impact upon recharge in the BSZ.

Silva and Clarke (2002) validated SLEUTH's portability in a European setting, where urban development patterns tend to differ from those found in the U.S. Urbanization of two Portuguese cities--Lisbon, and Porto, was simulated for 25 years into the future. Despite the cities having different layouts and general topography, SLEUTH was successful in recreating past urban extents in calibration for both cities, and substantial improvement in model performance was reached in terms of accuracy. Lisbon presented a more regular transition between calibration stages, meaning the values tended to adjust to local characteristics gradually, while Porto, due to its distinct landscape characteristics, showed an increase in performance in latter calibration stages when the model became more sensitive to the actual pattern of urbanization (Silva & Clarke, 2002). Dietzel and Clarke (2004) further examined SLEUTH simulation by first reproducing extents in San Joaquin County, CA, and later used three synthetic datasets to test SLEUTH calibration (2007). By combining previously used metrics into one, the Optimal Sleuth Metric (OSM), they answered a lingering question regarding the optimal SLEUTH calibration routine. Generally, there are three methods for simulating different scenarios of urban growth in the SLEUTH model (Rafiee et al., 2009). The first is by changing the final growth parameter values derived in calibration to project certain types of growth like 'compact', 'infill', or 'extensive' (Bihamta et al., 2014; Dezhkam et al., 2013; Goodarzi et al., 2016; Mahiny & Gholamalifard, 2007; Rafiee et al. 2009; Sakieh et al., 2014a; Sakieh et al., 2014b). The second, through weighting the exclusion layer,

where a range of protection values are assigned to different features and their buffer zones, often in conjunction with an analytical hierarchy process and multi-criteria evaluation (Mahiny & Clarke, 2012; Sakieh et al., 2015; Sakieh & Salmanmahiny, 2016). Finally, the third, by modification of SLEUTH's self-organizing constraints, such as the thresholds and multipliers for boom/bust cycles or the critical slope value--the average slope value at which the system increases the spread parameter (Yang & Lo, 2003). Of these methods, the first seems to be the most widely applied throughout the literature, with the second and third methods following respectively. Scenario outcomes are compared to 'historical' growth scenarios, where SLEUTH is allowed to run unaltered to establish a baseline of future urban extent. Guan and Rowe (2016) used the first method of scenario creation to examine four possible growth trajectories along the Changjiang River Delta. Scenarios included 'development corridors', 'development corridors plus big city growth', 'environmental system concerns, plus development corridors' and 'disaster prevention, plus development corridors.' Development corridors are geographic areas of high priority to planners and public officials, as they represent catalysts for economic growth. They can be likened to the BSZ, as Austin developers seek to capitalize off its natural beauty and resources for economic gain. By altering SLEUTH source code, the authors added a new variable to the prediction algorithm to incorporate the type of growth taking place, where important features of environmental systems such as forests and protected lands held priority over development corridors. If a conflict occurred between development and a feature, the development corridor cell was reduced to zero, disallowing all future growth and preserving environmental integrity and sustainable growth outcomes, much like the impervious cover limits of the SOS Ordinance.

Liu et al. (2020) used the second method of scenario creation to examine the influence of ecological source, corridor, and security patterns on future environmentally sustainable growth in Quanzhou, China. The ecological security patterns (ESP) of four different environmental factors including water, geology, biodiversity, and recreation, were integrated into three different exclusion layers of Basic ESP, Intermediate ESP, and Optimal ESP. Regarding hydrology, features such as rivers and lakes, flood storage area, and inundation area were applied buffers, where shorter buffers carried higher weights to offer more protection from development. The maximum value allowed in each exclusion layer corresponded to the amount of overall protection from urbanization the layer offered, where higher maximum values offered more protection. The maximum value allowed in the basic protection scenario was equal to 1.0, intermediate equal to 2.0, and optimal equal to 3.0. They found that the basic scenario projected the largest amount of urban growth, while the optimal scenario projected the least. The optimal scenario also showed the least amount of penetration into forests, grasslands, and wetlands, but the development that did take place was often small and fragmented, therefore resulting in less efficient urban systems. This presents a paradox, where protective measures that aid in the preservation of a given hydrologic feature(s) often cause changes elsewhere in a hydrologic system and can undermine the long-term goal of sustainable development through policy.

Finally, Xiang and Clarke (2003) summarized the various facets that make up sound land-use modeling scenarios. Land-use scenarios are synthesized hypothetical snapshots of patterns that may result from the implementation of plans, policies, or regulations (Xiang and Clarke, 2003). A good scenario should serve a 'dual function' by

first bridging the gap between land-use modelers and model users (usually planners, stakeholders, or the public), then stretching the imaginations of users to see the bigger picture behind modeling exercises, including underlying causality, alternative outcomes, and thematic possibilities. There are five common components to land-use scenarios. How the modeler leverages them to portray a given policy determines the model's effectiveness at depicting plausible outcomes to urban and hydrologic systems. They are *alternatives* – the potential plans, policies, or regulations to be simulated; *consequences* – the cumulative effects each alternative has upon future land-use; *causations* – the relationships between alternatives and consequences; *time frames* – the period between the implementation of an alternative and the consequence; and *geographical footprints* – the spatial patterns of alternatives and consequences.

Together, these components make up three key credentials that scenario simulation should possess: 1) *Plausible unexpectedness* states that a good scenario should not merely state the obvious nor confirm what is already known. Instead, it should seek to 'creatively incorporate the considerations of low-probability—even wildly imaginative—outcomes' through the incorporation of diverse perspectives, innovative roles for agents, and comprehensive summations of agent interactions, while maintaining a credible storyline (Xiang & Clarke, 2003); 2) *Informational vividness* engages a model user by presenting information in such a way that an emotional connection is made between the user and model content, theme, and spatio-temporal context; and 3) *Cognitive ergonomic design* ensures the scenario is easily digestible by the user by the appropriate use of single- or multi-themed scenarios of proper size regarding the number of variables or agents, and by choosing an appropriate timeframe to simulate. Perhaps

counterintuitive, model simplicity is a key factor for incorporating these components. Therefore, comparing current SOS guidelines with realistic policy alternatives that capture Austin’s future social and economic climates through urban expansion may result in vivid insight into unexpected impacts to BSZ hydrology that stakeholders can easily understand and incorporate into future plans.

2.3 Overview of Groundwater Modeling

Groundwater is deeply connected to the entire hydrosphere, among other Earth spheres, therefore many concepts and methods are used to model aspects of an aquifer system. Groundwater modeling provides a quantitative framework for synthesizing field information and conceptualizing hydrogeologic processes (Beddows, 2016). There exist three basic types of groundwater models. The first, *physical* groundwater models, are scaled down three-dimensional, tangible objects that demonstrate the processes and properties of an aquifer in action. Scientists build physical models to study aquifer characteristics that are otherwise inaccessible to the human eye.

Next, *conceptual* groundwater models are expressions of an aquifer that represent an idealistic rendering of aquifer processes, properties, and many times, regional relationships with adjacent bodies of rock. These conceptualizations build upon the physical information derived from the former to create *numerical* groundwater models. Numerical models are mathematical representations of an aquifer that are almost always created, computed, and displayed on a computer. They represent the synthesizing agent by which field data and theoretical notions about an aquifer are leveraged to make quantitative predictions about groundwater.

There are three spheres of general topics in groundwater modeling—recharge,

vadose zone hydrology, and saturated zone hydrology. Although each sphere pertains to a distinct location upon or below the earth, their relationships to one another resemble a Venn diagram, where each sphere partially relies upon data, concepts, or literature in another, thus creating overlap in methods, research design, and often, relevant conclusions (Park et al., 2021; Wu et al., 2021).

In the recharge sphere, authors have taken to topics such as delineating potential recharge areas (Ali Rahmani & Chibane, 2018), or quantifying the distribution and impacts of artificial recharge to a groundwater system (Abraham et al., 2021; Alkhatib et al., 2021), man-made alterations to physical aquifer properties through artificial recharge (Chu et al., 2019), and the impacts of LULC on groundwater levels (Ainiwaer et al., 2019). GIS plays a valuable role in these endeavors, especially when LULC is involved. One of the most widely used techniques for simulating the effects of LULC change on groundwater is by integrating future LULC projections with physical-based hydrologic models. Dams et al. (2008) linked a Conversion of Land-Use and its Effects at Small regional extent (CLUE-S) model to a Water and Energy Transfer between Soil, Plants, and Atmosphere under quasi-Steady State (WetSpass) groundwater recharge model for four scenarios of LULC change based on future land-use demand, present land-use trends, and spatial policies and restrictions. Results showed a clear link between LULC and the amount of aquifer recharge in all scenarios tested.

Other authors have taken to developing in-house CA models that leverage the physics-based flow equations of more robust hydrologic models. Kassogu e et al. (2017a) used elevation, soil type, and LULC to inform the Two Scale Cellular Automaton for Flow Dynamics model (2CAFDYM), which linked to climate data of annual mean

temperature and average annual precipitation to test baseline, pessimistic, and optimistic scenarios of future recharge, runoff, and evapotranspiration quantities (Kassogu e et al., 2017b). The optimistic scenario projected the lowest rate of urban growth, whereas the pessimistic projected the most, and baseline, a continuation of the contemporary growth trend. They found a decrease in aquifer recharge for the pessimistic scenario, an increase in recharge for both the optimistic and baseline scenarios, and all three scenarios saw an increase in evapotranspiration.

Regarding established methods, the Soil Water Assessment Tool (SWAT) is often used to simulate impacts to hydrology from impervious cover. Sunde et al. (2016) integrated three projected scenarios of impervious cover derived by the Impervious Change Analysis Tool (I-CAT) with additional inputs of elevation, soil type, precipitation, temperature, and streamflow observations to SWAT to estimate future impacts to runoff, baseflow, and evapotranspiration. They observed an increase in both runoff and baseflow, with a decrease in evapotranspiration, as impervious surface expanded. Wang et al. (2021b) combined delineations of past impervious cover patterns in an urban watershed with SWAT to determine its impacts on water balance components and found that an increase of 17% impervious area led to a 20% increase in the urban surface runoff ratio. Li et al. (2019) coupled impervious cover scenarios derived by the CA-Markov model with SWAT to predict changes in recharge, runoff, baseflow, and evapotranspiration. They found that changes to LULC significantly impact annual and monthly averages of streamflow, that forests reduce peak flow and runoff in flood season while increasing infiltration, and that future expansion of impervious cover is expected to increase runoff and wet season flow, leading to more frequent flooding and a decrease in

evapotranspiration and baseflow.

Another well-established method of hydrologic modeling is the U. S. Geological Survey (USGS) SWB tool. SWB is widely used because of its adaptability to different environmental and geological settings, open-source access, and simplicity of inputs. Mair et al. (2013) computed aquifer recharge and water balance components for the South Korean Island Jeju using baseline, drought, and climate-LULC scenarios through 2009 and found that results were within the range of previous studies in the area, concluding that SWB provides a robust and valid means of calculating recharge. Shuler et al. (2021) combined the SWB2 model with a general circulation climate model to predict future recharge on a volcanic island. It was found that, currently, 57% of rainfall on the island recharges the aquifer, and though this number may increase in the future, impervious surfaces were shown to have a negative impact on its outcome. In addition to these exotic locations, SWB has been used to estimate recharge in more common settings throughout the United States, including North Carolina (Antolino, 2022), the Grand Canyon (Knight, 2022), Oregon (Corson-Dosch & Garcia, 2022), Maine (Nielson, 2019), Florida (Nardi, 2018), and the Mississippi Embayment aquifer system straddling Louisiana, Mississippi, Arkansas, Alabama, Tennessee, Kentucky, and Missouri (Westenbroek et al., 2021), showing the model's versatility.

A specific application that is clearly lacking in the groundwater modeling literature and, thus, worthy of exploration is the integration of CA-derived urban growth patterns with the SWB model. Although both methods show histories of clear justification for their widespread use, they have yet to be combined, and doing so may result in new insights in both the recharge modeling domain, as well as the policy domain

regarding Austin's SOS Ordinance. Results of such a study might boost the confidence of citizens, policymakers, and stakeholders in their decisions about whether to expand or decrease SOS regulations, and conclusions may also be drawn about its past effectiveness at protecting the aquifer from the harms posed by urban development.

2.4 Case Studies in Urban Policy, Growth, and Hydrology

The dynamic relationship between policy, growth, and hydrology is difficult to quantify and can be complicated by urban settings. As more agents and stakeholders become involved in the policy making and implementation process, the rate and magnitude of LULC change is more drastic. Moreover, the role of impervious cover in these myriad relationships impacts urban hydrology in wider ranging and more profound ways than in rural settings. Ghimire and Johnston (2013) applied the SWAT model to urban, agricultural, and rural control watersheds in the southeastern United States to gain insights into the impacts of rainwater harvesting policies on runoff for urban and agricultural scenarios. Baseline, urban rainwater harvesting, agricultural rainwater harvesting, and urban plus agricultural rainwater harvesting scenarios were composed of variables that reflected policy adoption rate, watershed population density, LULC, runoff reduction, water supply reliability, design constraints, and cost in simulating storage reservoirs along hypothetical harvesting networks (Ghimire & Johnston, 2013). A hypothetical adoption rate of 100% decreased runoff by up to 16%, while an adoption rate as low as 25% reduced it by 6%, demonstrating the significant impact policy can have on watershed hydrology. During the non-growing season, urban rainwater harvesting was shown to have the highest impact on runoff due to the large amount of impervious surface area in the urban watershed, reflecting the compounding effects that

policy and urban growth can have on a hydrologic system.

In contrast to this explicit urban scenario, Gomes et al. (2021) studied the impacts of climate change and LULC on runoff in a tropical Brazilian agriculture watershed. Despite the non-urban setting, ‘green road’ and ‘fossil fuel’ scenarios simulated a conservative urbanization policy for impervious cover addition that encouraged gradual and sustainable development through afforestation, and a more aggressive policy that encouraged rapid development through deforestation. Although climate was found to be the biggest factor in increased runoff, controlling for variation in precipitation resulted in the LULC changes of the fossil fuel scenario showing a significantly higher increase in runoff, and decreases in soil water and evapotranspiration compared to historical trends and the green road scenario. In the long-term simulation (i.e., 2045), LULC changes have the highest correlation with variation in hydrologic system components. This demonstrates the direct link between urbanization policy and hydrology, and that even in a not-yet-fully urbanized location, poor policy formulation and implementation can have significant impacts on watershed dynamics.

As a synthesis of this concept, and similar to the scale of investigation used in this study, Wright et al. (2021) explored the hydrologic response of an urbanizing watershed near Portland, Oregon to urbanization policies. They used an ensemble of process models within the Envision framework (Bergström & Lindström, 2015) to evaluate the effectiveness of 50-year policy scenarios, including ‘stressed resources’ and ‘integrated water future’, which simulated lagging water protection policy and action caused by rapid growth combined with poor planning and implementation, and an anticipatory planning approach operating at the watershed-scale that allows for adaptation to obstacles and

rapid change, respectively. Results showed that the primary impact of urbanization on hydrology in both scenarios was a reduction in evapotranspiration and increased streamflow caused by an increase in runoff, and that conservation of upland forests and riparian buffer zones prevents this increase. The current SOS Ordinance addresses these preventative measures, however, it is not clear from this particular case study, the degree to which upland forests and riparian zones must be protected from impervious cover.

2.5 Case Studies in Central Texas

Several case studies looking to assess urban development in central Texas have taken place in recent years, with one specifically dedicated to assessing the SOS Ordinance. Sung, Yi, & Li (2013) investigated urban development patterns before and 16 years after SOS enactment. They compared patterns in the Williamson Creek (WC) subwatershed of the RZ to patterns in five similar but less-regulated control subwatersheds in Austin using the lacunarity index. The control subwatersheds had limits of 30 – 45% impervious cover depending on land-use type, compared to 15% in WC. Results showed an overall increase of impervious cover in WC from 25% in 1991 to 52% in 2008. Prior to SOS enactment, urban development patterns in terms of the lacunarity index were similar across all subwatersheds. However, the 2008 index was significantly lower than the control average, meaning that development in WC had become more dispersed with fragmented forest areas, and all five control subwatersheds still held relatively large forest stands compared to WC. They concluded that the SOS Ordinance exasperated urban sprawl by encouraging developers to purchase more land along the urban fringe where prices are considerably lower and open space more available. Although they noted other factors might play a role as well, and hence

recommended that the ordinance be re-evaluated.

Kim et al. (2017) compared the impact of green space abundance on the amount of runoff in 82 watersheds throughout Dallas, Houston, San Antonio, and Austin MSAs for years 2007 and 2012 using two linear regression models to simulate variation of mean daily runoff depth as a function of the Normalized Difference Vegetation Index (NDVI). Control variables of average precipitation, soil porosity, drainage density, percentage of 100-year floodplain, mean slope, watershed elongation ratio, impervious cover, and wetland were employed alongside NDVI in an ordinary least squares (OLS) regression model for each year. The OLS results were subsequently compared against population-weighted densities, or the average density of census tracts, inside each MSA. Results of changes in census tract densities from 2007 to 2012 showed that Dallas, Houston, and Austin grew at a high rate, but that development had occurred along the urban fringe and near suburbs, whereas San Antonio showed more preferable compact growth concentrated in its urban core. Austin watersheds produced the least amount of runoff of all MSA's, but this may be due to locational bias of the study area, as samples were located outside of the inner city, contained a relatively low amount of impervious surface compared to other MSA's, and Austin's strict watershed protection policies. They found NDVI was the most important explanatory variable in the OLS regression for 2007, and second most important in 2012, behind impervious cover. They concluded that green space contributes to reducing surface runoff in the selected watersheds, and that all watersheds included in the study are rapidly decreasing in available green space, suggesting that more protection policies should be considered in each MSA. Although these results are significant to this study in terms of the impacts of green space on runoff,

there is still a need to study this relationship and its impact upon subsurface hydrology in greater detail and in an inner-city context.

Guerra & Debbage (2021) used data from the National Land Cover Database (NLCD) to quantify urban development along the I-35 corridor in central Texas. In contrast to previous central Texas case studies, they found that due to limited urban development since 2001, and a consistently declining rate of urbanization observed throughout the RC, protection policies seem to have been effective overall. However, Zhao et al. (2020) used LiDAR-derived 3-D maps to examine change in nine urban morphology types (UMTs) based on building densities and heights from 1992–2016, then examined UMT transitions year over year between four discrete time steps to determine the underlying processes that have contributed to Austin’s present urban form. They found that despite observable infill expansion from 1992 - 2001, with slightly less infill from 2006 - 2011, edge expansion was the predominant process that took place in all time periods, and that an observed increase in urban development in Austin is a consequence of sparsely built and transportation patterns, thus strengthening the argument that Austin has seen less desirable growth in the form of urban sprawl since the adoption of the SOS Ordinance. Therefore, previous research on this topic in Austin has found that despite the overall effectiveness of SOS in limiting impervious cover, it has encouraged urban sprawl and exacerbated the possible impacts of urban development upon BSZ hydrology.

In all case studies, the authors agree that more research regarding the effectiveness of the SOS Ordinance, and Austin’s urban development policy in general, is needed. Some suggest calculating direct and indirect costs and benefits from protection policies (Kim et al. 2017), or the impacts of regulation on hydrology or development

pattern (Sung, Yi, and Li 2013). Because many of these case studies included portions of study areas outside SOS jurisdiction, directed research into the ordinance's long-term impact upon BSZ hydrology, specifically, is needed to better assess its outcome. This research seeks to fill the gap in both urban and groundwater modeling literature regarding the integration of the SLEUTH and SWB models, as well as the need for further investigation into the impacts of the SOS Ordinance on BSZ hydrology.

3.0 MATERIALS AND METHODS

3.1 Study Area

Austin is located in central Texas (Figure 1), just east of the Balcones Escarpment, where the Blackland Prairies and Gulf Coastal Plains of east Texas meet the rolling hills of the Edwards Plateau to the west. It lies along the IH-35 corridor, 130 km northeast of San Antonio, and its city limits encompass an area of 834 km². This unique location along the foot of the escarpment places Austin in the Balcones Fault Zone, a belt of largely normal faulting that formed 20 - 25 million years ago that runs from Del Rio on the southwestern border northeast to Dallas (Bureau of Economic Geology, 2021). This faulting caused the Edwards Limestone to fracture which offered pathways for surface and groundwater to dissolve the present-day cavities that make up the Edwards RZ. Beyond the escarpment to the west lies the Texas Hill country, and the Edwards CZ, where water drains into stream and river channels that then cross the RZ and can lose all or much of their water to the Edwards Aquifer.

Tucked away in the southwestern corner of Austin is the BSZ (Figure 1). Its area covers 336 km², and spans portions of six watersheds-Little Barton, Barton, Williamson, Slaughter, Bear, and Little Bear. The BSZ straddles the Edwards contributing and recharge zones, with the recharge zone running in a linear fashion in the lower portions of Barton, Williamson, Slaughter, and Bear watersheds, and the upper portion of Little Bear, while Little Barton lies solely within the contributing zone and contains only a small portion of the BSZ. The total area of these watersheds is equal to 534 km² and serves as the study area for this research. Rainfall in BSZ watersheds eventually discharges at Barton Springs. Historically, the eastern portion of the BSZ has seen more urban

development, as it's closer to the IH-35 corridor and other major Austin thoroughfares, but as demand for commercial and residential development, and transportation infrastructure increases in the coming years, the largely undeveloped portions of the western BSZ are prone to new development.

There are three characteristics of the BSZ that make it a good candidate for this study:

- The BSZ is a peri-urban zone of transition between Austin and the rural Hill Country. This less urbanized setting provides the room and resources many endemic plant and animal species need to grow, and offers recreation, scenic views, and exposure to nature that Austin cannot.
- The extremely high permeability and hydraulic conductivity of the BSZ RZ make it an extraordinarily sensitive area for urban development. Impervious cover provides pathways for pollutants to be transported into the aquifer quickly and can pollute the many creeks and watering holes that Austinites frequent throughout the year.
- Despite the high productivity of the Edwards Aquifer, Texas is becoming more prone to drought (Texas A&M University, 2020). As Austin's population and freshwater demand increases over the coming decades, the BSZ provides a well-suited area for natural recharge to reach the aquifer and support that demand. The SOS Ordinance, and its restrictions to impervious cover in the BSZ, offers a chance to cap development that might preclude the support of the aquifer for future generations.

Combined, these unique characteristics of the BSZ provide an opportunity for interesting

scenario development for studying the impacts of impervious cover on BSZ hydrology and the efficacy of the SOS Ordinance in minimizing those impacts.

3.2 Urban Growth Model Data and Pre-processing

The SLEUTH urban growth model takes six greyscale images in gif format as input: urban extent, transportation, areas excluded from urbanization, slope, and hillshade. The sixth layer, land-use, is optional and is not used in this study. All images were projected to Universal Transverse Mercator zone 14N (meters) and carry a 30 m spatial resolution. Images were buffered and clipped to a distance of 8 km outside the study area to allow SLEUTH to simulate urban growth without adverse edge effects. The minimum data requirements to run the model are four discrete time periods of urban extent and two discrete time periods of transportation network.

3.2.1 Urban

Landsat 5 and 8 images (Figure 2) at 30 m spatial resolution were downloaded and processed to derive urban extents for years 2005, 2010, 2015 and 2022. Captures during leaf-off months were chosen, as this provides more opportunity to accurately delineate existing urban development due to less foliage. Cloud-free and approximate anniversary images were downloaded from the USGS EarthExplorer website, and a supervised Maximum Likelihood Classification (MLC) algorithm was used to classify both urban and non-urban pixels for each year using ERDAS Imagine version 16.6. The MLC training classes consisted of 75 training samples each. Urban samples included pixels containing various building materials like concrete, asphalt, roofing, and glass, while non-urban training pixels consisted of earth materials like water, grass, tree canopy, and natural wood. The type of impervious surface was not distinguished in the MLC

algorithm. Confusion matrices and kappa statistics were generated to assess the accuracy of each year's MLC, where only those results showing a kappa score of at least 0.70, or a 70% match between predicted and observed urban pixels were used in the urban growth model. The same images were used for both the collection of training samples and for the accuracy assessment. A stratified random sampling technique was used for the accuracy assessment, where 100 random sampling locations were chosen for each of the three classes output by the algorithm

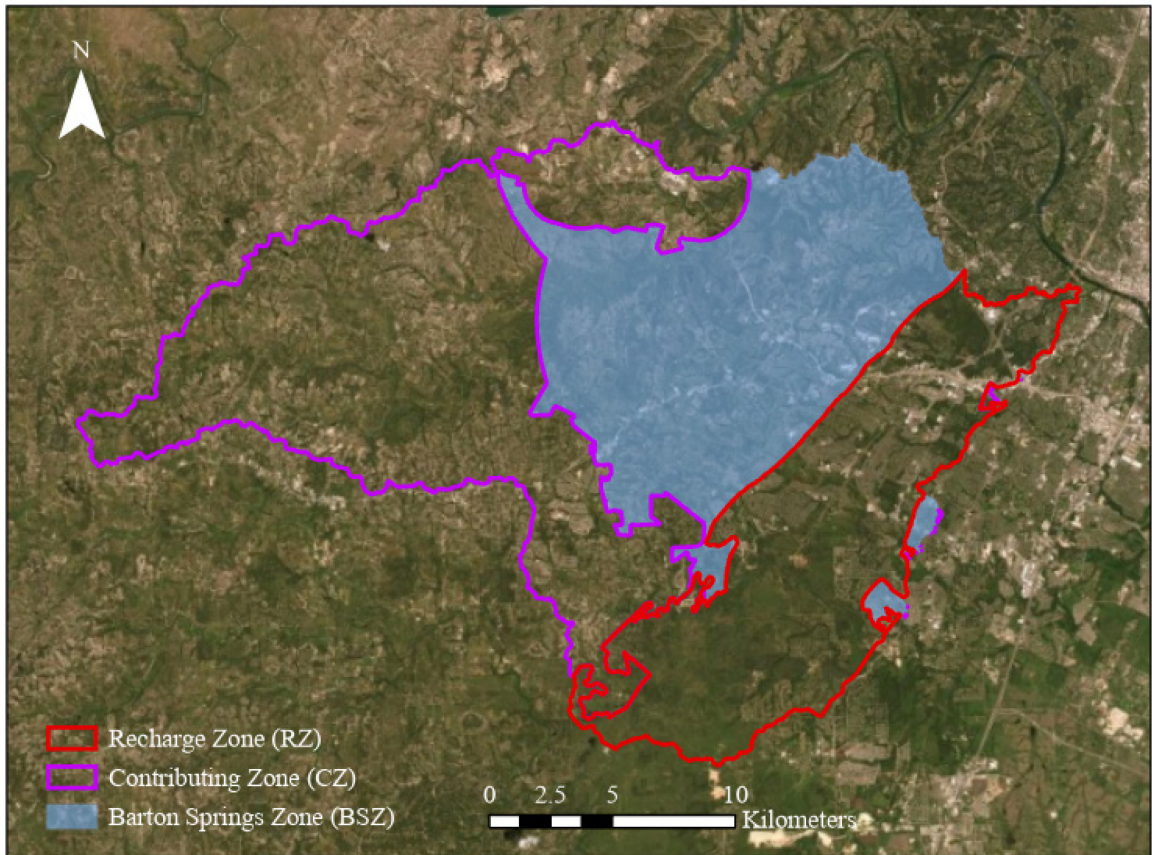


Figure 2. Landsat 8 imagery of the study area.

3.2.2 Transportation (Roads)

The transportation layer is used by SLEUTH for determining the affinity of new urban growth for road infrastructure. Transportation data were downloaded from the Texas Department of Transportation (TxDOT) data portal for 2011 and 2022. Roads were

classified into three classes, where large regional or state highways are most attractive to new growth, secondary feeder roads are neutral in attraction, and local primary roads are least attractive to new growth. The vector data were then rasterized into an array of cells representing the extent of transportation infrastructure for model input.

3.2.3 *Exclusion*

The exclusion layer represents areas that are unavailable to urbanization by SLEUTH. This includes areas such as waterways, parks and reserved open spaces, easements, and in the case of BSZ watersheds, two riparian buffers known as the Critical Water Quality Zone (CWQZ) and the Water Quality Transition Zone (WQTZ). Established by Section 1.5.2 of the City of Austin - Environmental Criteria Manual (City of Austin, 2022b), the CWQZ consists of the 100-year fully developed floodplain, bounded by various buffer widths for minor, intermediate, and major waterways, depending on the contributing drainage area of the waterway (Table 1). The WQTZ is adjacent to the outer boundary of the CWQZ and also carries various buffer widths depending on the waterway classification. Additionally, the main stem of Barton Creek is prescribed a 400 m buffer throughout the Barton watershed. Park and open space data were downloaded from the COA, CAPCOG, Travis County, and Texas Parks and Wildlife data portals, and 30 m exclusion buffers were applied to all parks, easements, and roads to create a more realistic development pattern.

Table 1. Prescribed waterway classification criteria and stream buffer sizes as prescribed by the City of Austin – Environmental Criteria Manual (City of Austin, 2022b).

Waterway Classification	Contributing Drainage Area (acres)	CWQZ Stream Buffer Size (feet)	WQTZ Stream Buffer Size (feet)
Minor	64 - 320	50 – 100	100
Intermediate	320 - 640	100 – 200	200
Major	> 640	200 - 400	300

3.2.4 Slope

The slope layer is used to establish the resistance of new growth to forming on steep hillslopes. A 7.5-minute digital elevation model (DEM) of 30 m spatial resolution was downloaded from the USGS National Map website, and a percent slope layer was created for input to SLEUTH using ArcGIS Pro 2.5.

3.2.5 Hillshade

The hillshade layer serves no functional purpose for computing new urban growth in the SLEUTH model. Instead, it provides a static background image for outputs to be displayed upon, giving spatial context to changes in urban extent over time. This layer was also derived from a 7.5-minute DEM of 30 m spatial resolution.

3.3 SLEUTH Model Calibration

Calibration is possibly the most important phase of building a sound predictive model (Dietzel and Clarke, 2007). SLEUTH is calibrated in three phases. The *coarse* phase uses inputs resampled to 120 m; the *medium* phase uses data resampled to 60 m; and the *fine* phase uses data at the original spatial resolution of 30 m. This data resampling saves computation time during brute force calibration and is the reason why the model requires at least four discrete time periods of urban extent for the study area,

where each year acts as a calibration node. SLEUTH calibration begins by using the oldest time period of MLC-derived urban extent to predict changes in urban growth until the number of iterations, or years, reaches that of the next node, completing one growth cycle.

At the end of each growth cycle, calibration metrics are used to analyze which combination of growth coefficients best predicted the urban extent of the end node. Calibration metrics include the *compare* statistic – the ratio of the number of modeled urban pixels to the number of observed urban pixels; *population* – Pearson’s r^2 for modeled urbanization compared to observed urbanization; *edges* – Pearson’s r^2 for modeled urban edge cell count and observed urban edge cell count; *clusters* – Pearson’s r^2 for modeled urban clustering and observed urban clustering; *cluster size* – Pearson’s r^2 for the average modeled urban cluster size and the average observed urban cluster size; the *Lee-Sallee shape index* – a measurement of spatial fit between modeled growth and observed growth; *% urban* – Pearson’s r^2 for percent of available pixels urbanized compared to observed urban pixels; *slope* – Pearson’s r^2 for the average slope of modeled urban cells compared to the average slope of observed urban cells; *x-mean* – Pearson’s r^2 for the average x-value of modeled urban cells compared to the average x-value of observed urban cells; *y-mean* – Pearson’s r^2 for the average y-value of modeled urban cells compared to the average y-value of observed urban cells; and *rad* – Pearson’s r^2 of the standard radius of the urban distribution (Dietzel and Clarke, 2007). In this study, the product of the compare, population, edges, clusters, slope, x-mean, and y-mean metrics was used to create the OSM (Equation 1) for calibration.

$$OSM = Compare \cdot Population \cdot Edges \cdot Clusters \cdot Slope \cdot X\text{-mean} \cdot Y\text{-mean} \quad (1)$$

3.4 Hydrologic Model Data and Pre-processing

The SWB model takes four gridded datasets in ASCII format as inputs: hydrologic soil group, LULC, available soil-water capacity, and surface water flow direction. In addition to these data, the model requires daily climatological data in grid format: average precipitation (in inches), maximum ambient air temperature (in degrees Fahrenheit), and minimum ambient air temperature (in degrees Fahrenheit). Last, two lookup tables must be provided to the model to assign Natural Resource Conservation Service (NRCS) runoff curve numbers, interception values, rooting depths (in feet), and maximum daily recharge values (in inches per day) to each combination of hydrologic soil group and LULC type (Westenbroek et al., 2010). The first contains Anderson Level II land-use classifications with associated soil parameters, and the second contains a Thornthwaite-Mather soil-water retention table that relates accumulated potential water loss to the amount of soil moisture retained for a range of soil-water capacities (Westenbroek et al., 2010). The first table was modified to provide LULC classes found in the study area integrated with SLEUTH model outputs of urban extents, along with corresponding runoff curve numbers, maximum recharge rates, and root-zone depths for relevant soil types within each land-cover, while the second table was provided with the SWB model download and was not modified from the original version.

3.4.1 *Soil Group*

Hydrologic soil group vector data were downloaded from the NRCS data portal and clipped to the study area before being rasterized in the GIS to derive the model input grid. There are four hydrologic soil groups ranging from A – D. “A” soils have a high infiltration capacity, thus a low chance of causing runoff, while “D” soils have a low

capacity for infiltration, thus a high potential for creating runoff (Westenbroek et al., 2010).

3.4.2 *LULC*

The LULC layer provides the opportunity to integrate SLEUTH urban growth model outputs into the SWB recharge model to examine the possible impacts to hydrology by various scenarios of impervious cover. The most recent (2019) NLCD LULC raster data was downloaded and clipped to the study area. The NLCD data was overlain with SLEUTH urban model projections for each respective scenario, and cells found to be projected to urbanize by SLEUTH were reclassified to the NLCD class ‘Developed, Medium Intensity’. Because SLEUTH does not differentiate the intensity of urbanization in its projections, this methodology offers the most objective way of assigning a LULC class to newly urbanized cells. The remaining NLCD cells not projected to urbanize by SLEUTH were unaltered to produce the final LULC input grid for each scenario.

3.4.3 *Soil-Water Capacity*

Soil-water capacity data were downloaded from the NRCS data portal in the form of a Microsoft Access database and spatially joined to the corresponding soil groups to produce the input grid.

3.4.4 *Surface Water Flow Direction*

The same DEM used to derive the slope, and hillshade layers in the SLEUTH model was used to attain a flow direction raster using the GIS. Prior to hydrologic modeling, the DEM was hydrologically conditioned through an iterative process of filling sinks, or closed depressions, burning streams, or slightly lowering the streambed

elevation to reinforce the correct flow pattern, and fencing ridges to reinforce local topographic maxima. This ensured that realistic drainage patterns are depicted by the flow direction grid, so an accurate flow model was computed by SWB.

3.4.5 Climatological Data

Daily climate data from January 1, 2011 through December 31, 2020 were downloaded from the PRISM climate group (Oregon State University, 2014) which uses an ensemble of interpolation techniques to derive daily climate grids for the contiguous United States. Climate grids were then reprojected and clipped to the study area.

3.4.6 Lookup Tables

The first lookup table is a tab-delimited text file derived by the user containing columns for land-use code, description, assumed imperviousness, the associated NRCS runoff curve number, maximum recharge rate, interception value, and root-zone depth for each soil type found in the study area. These data were downloaded from the NRCS data portal, where the downloaded table was imported to the GIS to join appropriate values to corresponding soil types and land-use type. The second lookup table is a tab-delimited text file provided with the SWB download and contains columns for available water (inches per foot), and root-zone (feet) for various combinations of soil type and vegetation found in the study area (Westenbroek et al., 2010).

3.5 SWB Model Calibration

The SWB recharge model was calibrated using the Rorabaugh method for baseflow separation (Rorabaugh & Simons, 1966). Baseflow separation is a technique that separates storm flow from baseflow in a stream hydrograph. Baseflow can be assumed to be equivalent to aquifer recharge. Streamflow records from January 01, 2011

to December 31, 2020 for four stream gages within the study area were analyzed for baseflow, and subsequent recharge rates were then averaged. The SWB model was then calibrated by altering curve numbers, maximum recharge amounts, and root zone depths in the land-use lookup table until the mean annual recharge value across the entire study area was within 10% of the mean recharge rate derived from the four stream gages by baseflow separation.

3.6 Urban Growth and Recharge Scenarios

Once calibrated, SLEUTH was allowed to project future urban extents in BSZ watersheds through the year 2042, where only the cells showing greater than a 70% probability to urbanize were chosen for further analysis. This 20-year window allowed sufficient growth cycles to pass so that robust predictions were made while maintaining a high degree of accuracy, as predictions become less accurate as time goes on. Within this time period, four different urban growth scenarios were simulated, where each scenario represents a different set of impervious cover restrictions as imposed by the SOS Ordinance.

The first scenario consisted of a baseline projection of urban growth in accordance with current SOS restrictions. In this scenario, impervious cover was limited to 15% of the RZ that falls within BSZ watersheds, 20% of the CZ that falls within the Barton watershed, and 25% of the remainder of the CZ within BSZ watersheds. The second and third scenarios represent hypothetical outcomes of urban growth based on variations of the current limits. The aggressive scenario consisted of 5% more restriction than those currently prescribed by the SOS Ordinance, in accordance with the changes proposed by the GEAA, while the conservative scenario consisted of 5% less restriction

than those currently prescribed by the ordinance. The terms ‘aggressive’ and ‘conservative’ were chosen to reflect the amount of action taken by the COA to limit impervious cover, where the aggressive scenario is equal to more restriction. Resulting scenarios of urban growth were then integrated into the SWB LULC input grid for their respective SWB model run to derive scenarios of possible changes to aquifer recharge due to changes in impervious cover limitations. Finally, an extreme scenario was simulated to demonstrate the outcome of a worst-case scenario, where the highest SLEUTH growth coefficients found in the top 10% of OSM scores were used.

The SOS Ordinance is currently enforced on a site-by-site basis at the parcel level, where a COA Environmental Inspector calculates the proportion of a given site that will be classified as impervious cover upon completion of the new construction to ensure that SOS limitations are met. The proportion of impervious cover is calculated on a net site area (NSA) basis (Table 2), as defined in Appendix Q-1 of the City of Austin – Environmental Criteria Manual (City of Austin, 2022c). NSA represents the total amount of land that is available for construction of impervious cover and is found by first computing total upland area (TUA), equal to gross site area (acres) minus acreage for the CWQZ and WQTZ riparian buffers. NSA is equal to 100% of all TUA where slopes fall between 0 – 15%, 40% of all TUA where slopes fall between 15 – 25%, 20% of all TUA where slopes fall between 25 – 35%, and 0% of TUA over 35% slope. These slope-based proportions are to discourage construction on steep slopes that are more prone to erosion and runoff. Additionally, it is recommended to subtract wastewater irrigation areas from gross site area, however, this calculation will not be accounted for in this study.

Table 2. Net Site Area calculation table taken from Appendix Q-1 of the City of Austin – Environmental Criteria Manual (City of Austin, 2022c).

1	GROSS SITE AREA	= _____	ACRES
SITE DEDUCTIONS			
2	CRITICAL WATER QUALITY ZONE (CWQZ)	= _____	ACRES
3	WATER QUALITY TRANSITION ZONE (WQTZ)	= _____	ACRES
4	WASTEWATER IRRIGATION ZONES	= _____	ACRES
5	DEDUCTION SUBTOTAL	= _____	ACRES
UPLAND AREA (GROSS SITE AREA MINUS DEDUCTIONS SUBTOTAL)			
6		= _____	ACRES
NET SITE AREA CALCULATIONS			
7	AREA OF UPLANDS WITH SLOPES 0-15%	= _____ X 100%	= _____ ACRES
8	AREA OF UPLANDS WITH SLOPES 15-25%	= _____ X 40%	= _____ ACRES
9	AREA OF UPLANDS WITH SLOPES 25-35%	= _____ X 20%	= _____ ACRES
10	AREA OF UPLANDS WITH SLOPES >35%	= _____ X 0%	= _____ ACRES
11	NET SITE AREA	= _____	ACRES

For each growth cycle, SLEUTH computes urban growth for an entire study area. Therefore, the model is incapable of simulating impervious cover limits at the parcel scale. Instead, impervious limits were enforced in the SLEUTH model at the RZ and CZ scale. For instance, the 15% limit currently prescribed for the recharge zone dictates that one SLEUTH model run be made solely for this zone, where once 15% of the zone became urbanized, a bust cycle was triggered, and urbanization slowed significantly. The same methodology was applied to the contributing zone and its respective limits.

Once each zone's projections were run, zones were clipped, and the zonal outputs merged to form projections of urban extent throughout the entire study area for each year through 2042, and for each scenario. Because this methodology involves a large amount of intermediate geoprocessing, a Python script was written to perform this task. Modifications were made to SLEUTH source code to enforce the bust cycle thresholds that represent impervious cover limitations. This partitioning of zones for respective

model runs does not pertain to the SWB model. Additionally, slope thresholds used to compute NSA were embedded in the SLEUTH exclusion layer by randomly selecting BSZ raster cells within a given range of slope degree, vectorizing the proportion of that range not available to construction of impervious cover, then merging the vector outputs with other exclusion areas.

The efficacy of the SOS Ordinance on limiting the impacts to aquifer recharge by impervious cover, and the possible impacts to recharge if those limits were to be altered, was examined by comparing SWB outputs of mean annual recharge for the extreme, conservative, and aggressive scenarios to the baseline scenario, respectively, using a pairwise Wilcoxon rank-sum test. Additionally, a Kruskal-Wallis test was used to test for significant difference among zones within each scenario, as well as to compare like-zones among scenarios. The null hypothesis employed in each test was that there is no significant difference in the aquifer recharge rate among the zones and urban growth scenarios.

4.0 RESULTS

4.1 SLEUTH Model Calibration Results

The results of the SLEUTH calibration routine are presented in Table 3. The number of iterations (NI) performed on the historical data totaled more than 18,000 to derive the best fit coefficients (BFC) for the baseline, aggressive, conservative, and extreme scenarios. The number of Monte Carlo Iterations (MCI) ranged between 5 – 9 per calibration phase. Total run time of SLEUTH calibration equaled 56 hours, with the Fine phase taking the longest amount of time to complete at 23.5 hours.

Table 3. Results of the SLEUTH calibration routine showing the best fit coefficients used in the baseline, conservative, and aggressive scenarios (BFC), and the best fit coefficients used in the extreme scenario (BFC extreme).

SLEUTH Calibration Coefficients								
Coarse			Medium			Fine		
MCI = 5			MCI = 7			MCI = 9		
NI = 3125			NI = 7776			NI = 7896		
OSM = 0.2919			OSM = 0.5381			OSM = 0.6827		
Growth Coefficients	Range	Step	Range	Step	Range	Step	BFC	BFC extreme
Diffusion	0 - 100	25	25 - 75	10	65 - 75	2	68	82
Breed	0 - 100	25	25 - 75	10	65 - 75	2	72	91
Spread	0 - 100	25	25 - 75	10	40 - 50	2	42	81
Slope	0 - 100	25	25 - 75	10	60 - 70	2	64	68
Road Gravity	0 - 100	25	50 - 100	10	70 - 80	2	75	86

4.2 SWB Model Calibration Results

The results of the SWB calibration routine are presented in Table 4. The annual mean recharge estimated by SWB was 13.13 cm, while the mean annual recharge estimated by baseflow separation across all four stream gages was 12.75 cm. Because each of the four stream gages used for calibration reside in watersheds with varying surface characteristics, and not all watersheds in the study area contain streamflow records, calibrating the mean annual recharge of the entire model domain to the mean annual recharge of all four stream gages was the most appropriate method for striking a

balance between accuracy and reality. The gages used for calibration are depicted in Figure 3.

Table 4. Results of the SWB calibration routine showing mean annual recharge values for stream gage sites used for calibration.

SWB Calibration Results		
USGS Site Name	Site Number	Recharge (cm/yr)
Barton Creek at Loop 360, Austin, TX	08155300	10.00
Williamson Creek at Oak Hill, TX	08158920	12.65
Slaughter Creek at FM 1826 nr Austin, TX	08158840	11.20
Bear Creek bl FM 1826 nr Driftwood, TX	08158810	17.14
	Mean	12.75
SWB Annual Mean Recharge (cm)		13.13

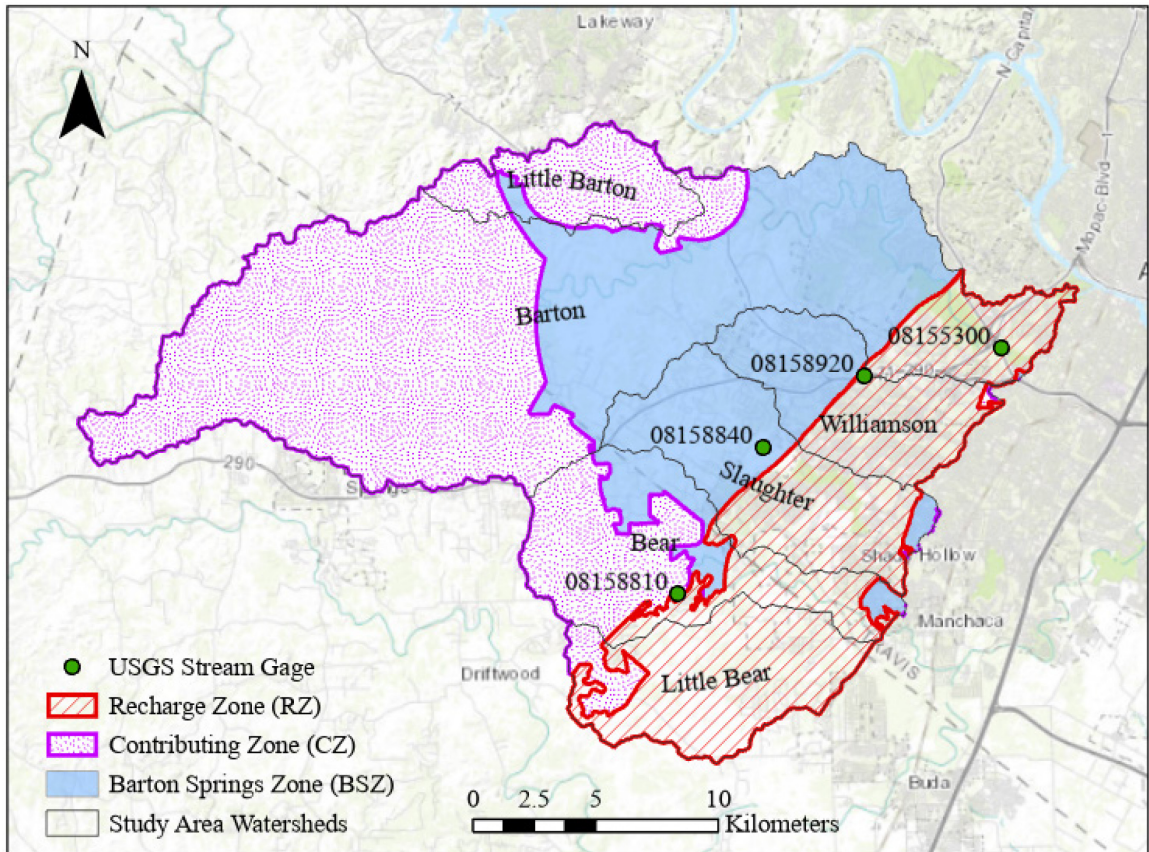


Figure 3. USGS stream gages used for calibration of the SWB model.

4.3 SLEUTH Model Results

4.3.1 *Current Land-Use*

For comparison, NLCD 2019 LULC data for the study area is presented in Figure 4. The total amount of urbanized area throughout the study area is equal to 4.60 km². In the portion of the BSZ lying within the CZ, the amount of urbanized area is equal to 1.56 km². In the CZ, the area urbanized is equal to 1.33 km², while in the RZ, the area urbanized is equal to 1.71 km². The results of all scenarios modeled by SLEUTH are within expectations regarding the relative amounts of area urbanized between scenarios based on the limit to impervious cover imposed in SLEUTH source code. Table 5 summarizes area calculations for all SLEUTH model scenarios. Table 6 summarizes the percent change in urbanized area between each scenario output and the NLCD 2019 LULC data.

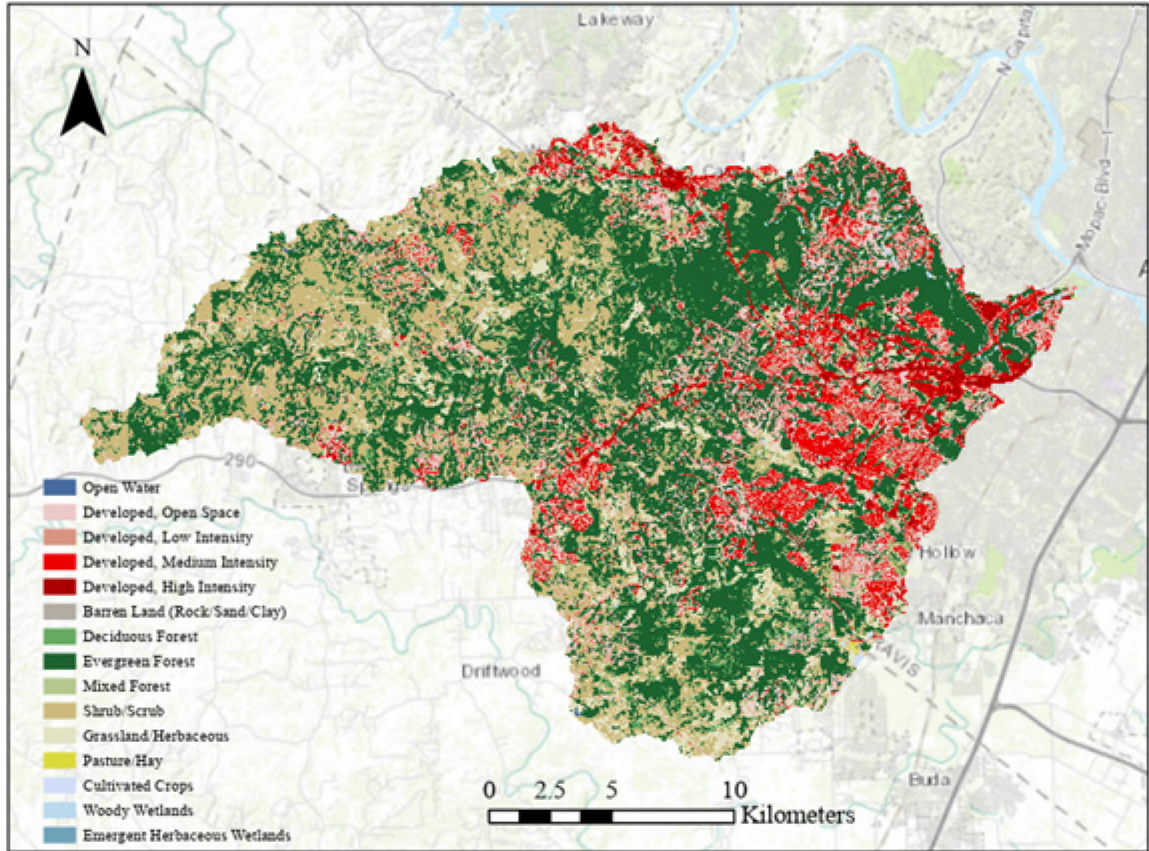


Figure 4. NLCD LULC 2019 data for the study area.

Table 5. Summary of area urbanized in the NLCD 2019 LULC data and area predicted to urbanize by SLEUTH through the year 2042 for each scenario.

Summary of Area Urbanized by SLEUTH				
Scenario	Area Urbanized (km ²)			
	Total	BSZ in CZ	CZ	RZ
NLCD 2019	4.60	1.56	1.33	1.71
Baseline	7.68	2.16	3.48	2.03
Extreme	9.25	2.56	4.37	2.31
Conservative	8.46	2.37	3.92	2.16
Aggressive	5.96	1.64	2.53	1.78

Table 6. Summary of the percent change in area urbanized between each SLEUTH scenario output and the NLCD 2019 LULC data.

Summary of % Change in Area Urbanized by SLEUTH				
Scenario	Change in Area Urbanized			
	Total	BSZ in CZ	CZ	RZ
NLCD 2019	-	-	-	-
Baseline	67%	38%	162%	19%
Extreme	101%	64%	229%	35%
Conservative	84%	52%	195%	26%
Aggressive	30%	5%	90%	4%

4.3.2 Baseline Scenario

The baseline scenario was simulated for years 2022 – 2042 using the BFC derived in the regular calibration routine. It represents urban growth through 2042 assuming the current trend with no action taken by the COA to alter the limits to impervious cover within the study area. The resulting urban growth predicted by the model is presented in Figure 5. The total amount of land predicted to urbanize throughout the study area in this scenario as of 2042 is equal to 7.68 km². In the portion of the BSZ lying within the CZ, the amount of urbanized area is equal to 2.16 km². In the CZ, the area urbanized is equal to 3.48 km², while in the RZ, the area urbanized is equal to 2.03 km².

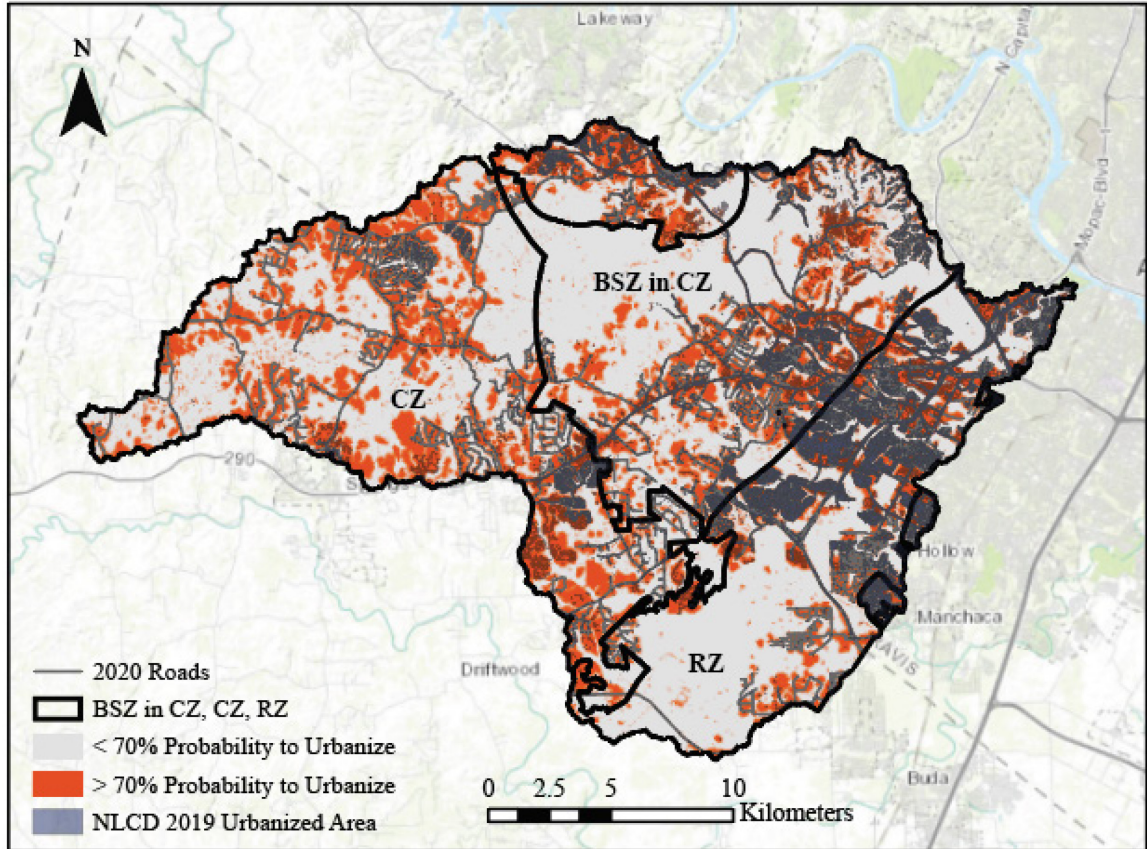


Figure 5. Urbanization as of 2042 as predicted by SLEUTH, urbanization as of 2019 in the NLCD 2019 LULC data, and the 2020 roads input layer for the baseline scenario.

4.3.3 Extreme Scenario

The extreme scenario was simulated for years 2022 – 2042 using the highest BFC found within the top 10% of OSM scores in the Fine phase of calibration. It represents extreme urban growth that may take place through 2042. The resulting urban growth predicted by the model is presented in Figure 6. The total amount of land predicted to urbanize in this scenario throughout the study area as of 2042 is equal to 9.25 km². In the portion of the BSZ lying within the CZ, the amount of urbanized area is equal to 2.56 km². In the CZ, the area urbanized is equal to 4.37 km², while in the RZ, the area urbanized is equal to 2.31 km².

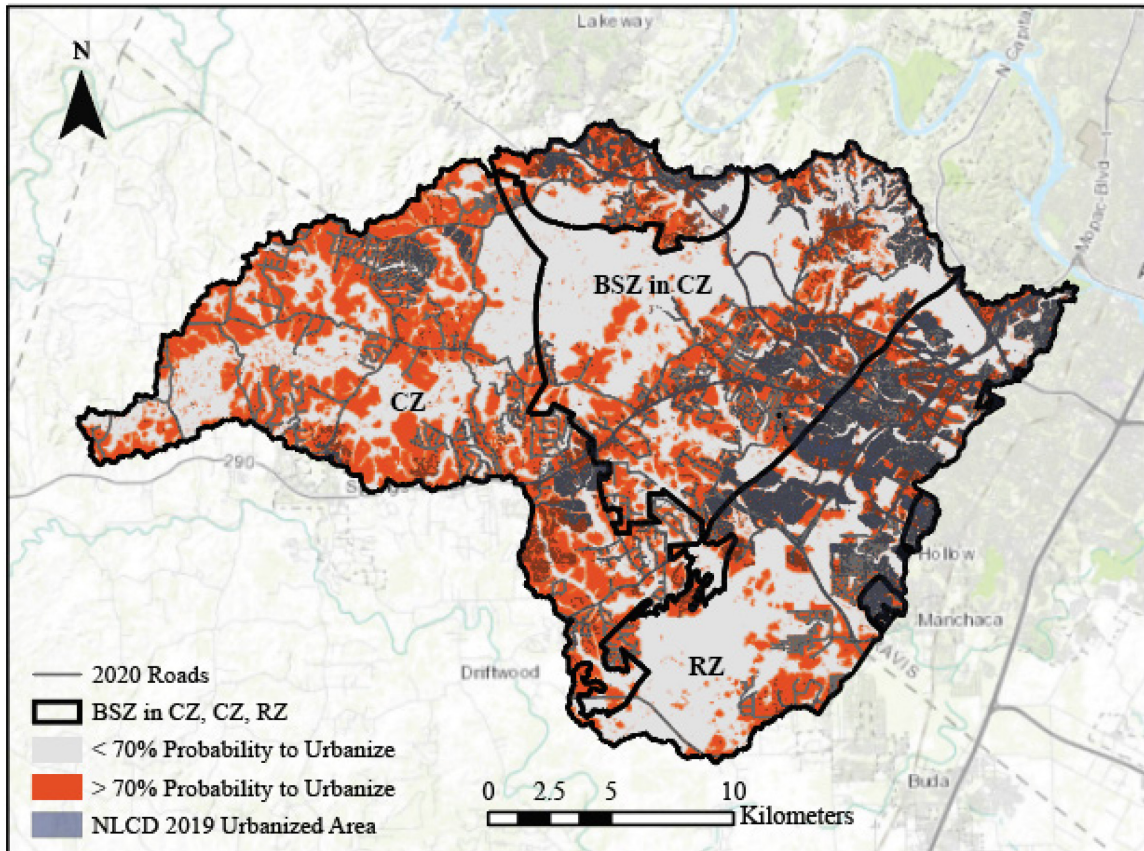


Figure 6. Urbanization as of 2042 as predicted by SLEUTH, urbanization as of 2019 in the NLCD 2019 LULC data, and the 2020 roads input layer for the extreme scenario.

4.3.4 Conservative Scenario

The conservative scenario was simulated for years 2022 – 2042 using the BFC derived in the regular calibration routine. It represents urban growth through 2042 if the COA applied a 5% reduction in restriction to impervious cover in each zone, therefore allowing for 20% impervious cover limit in the RZ, 25% impervious cover limit in the BSZ within the CZ, and 30% impervious cover limit in the CZ. The resulting urban growth predicted by the model is presented in Figure 7. The total amount of land predicted to urbanize in this scenario throughout the study area as of 2042 is equal to 8.46 km². In the portion of the BSZ lying within the CZ, the amount of urbanized area is equal to 2.37 km². In the CZ, the area urbanized is equal to 3.92 km², while in the RZ,

the area urbanized is equal to 2.16 km².

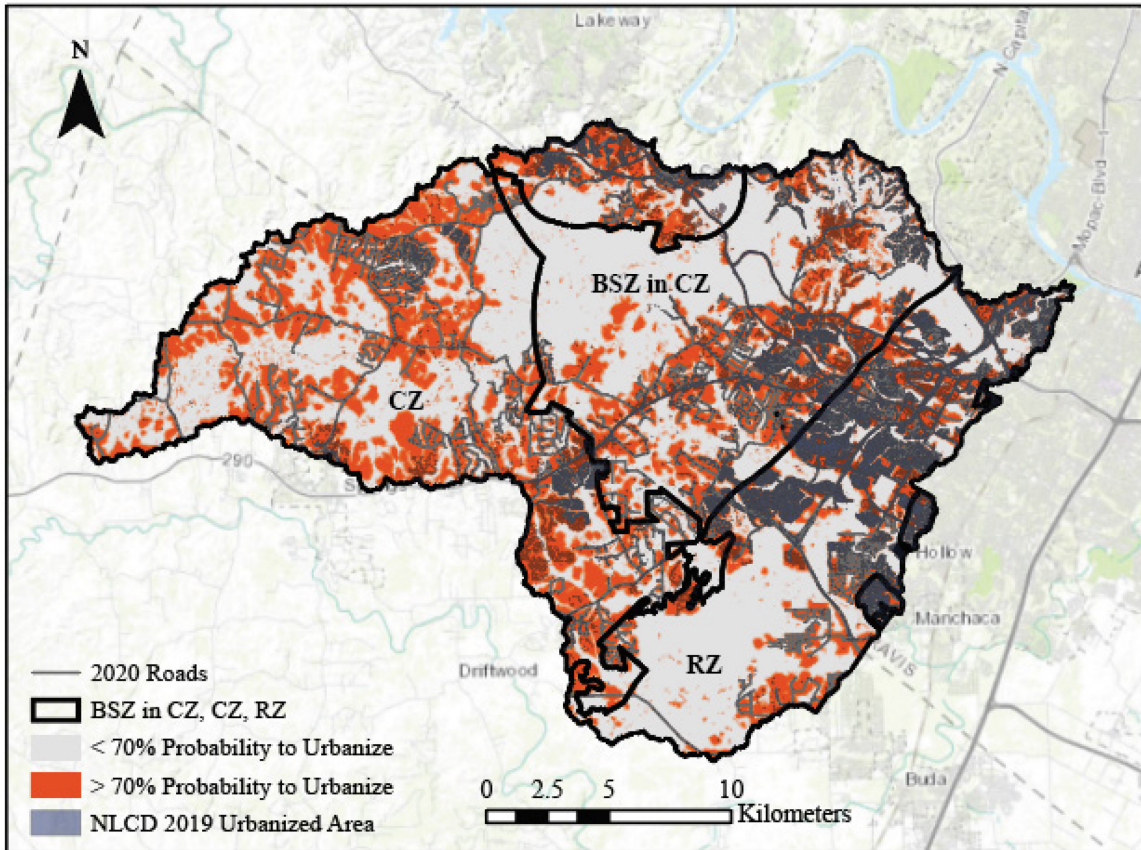


Figure 7. Urbanization as of 2042 as predicted by SLEUTH, urbanization as of 2019 in the NLCD 2019 LULC data, and the 2020 roads input layer for the conservative scenario.

4.3.5 Aggressive Scenario

The aggressive scenario was simulated for years 2022 – 2042 using the BFC derived in the regular calibration routine. It represents urban growth through 2042 if the COA applied a 5% increase in restriction to impervious cover in each zone, therefore allowing for 10% impervious cover limit in the RZ, 15% impervious cover limit in the BSZ within the CZ, and 20% impervious cover limit in the CZ. The resulting urban growth predicted by the model is presented in Figure 8. The total amount of land predicted to urbanize in this scenario throughout the study area as of 2042 is equal to 5.96 km². In the portion of the BSZ lying within the CZ, the amount of urbanized area is

equal to 1.64 km². In the CZ, the area urbanized is equal to 2.53 km², while in the RZ, the area urbanized is equal to 1.78 km².

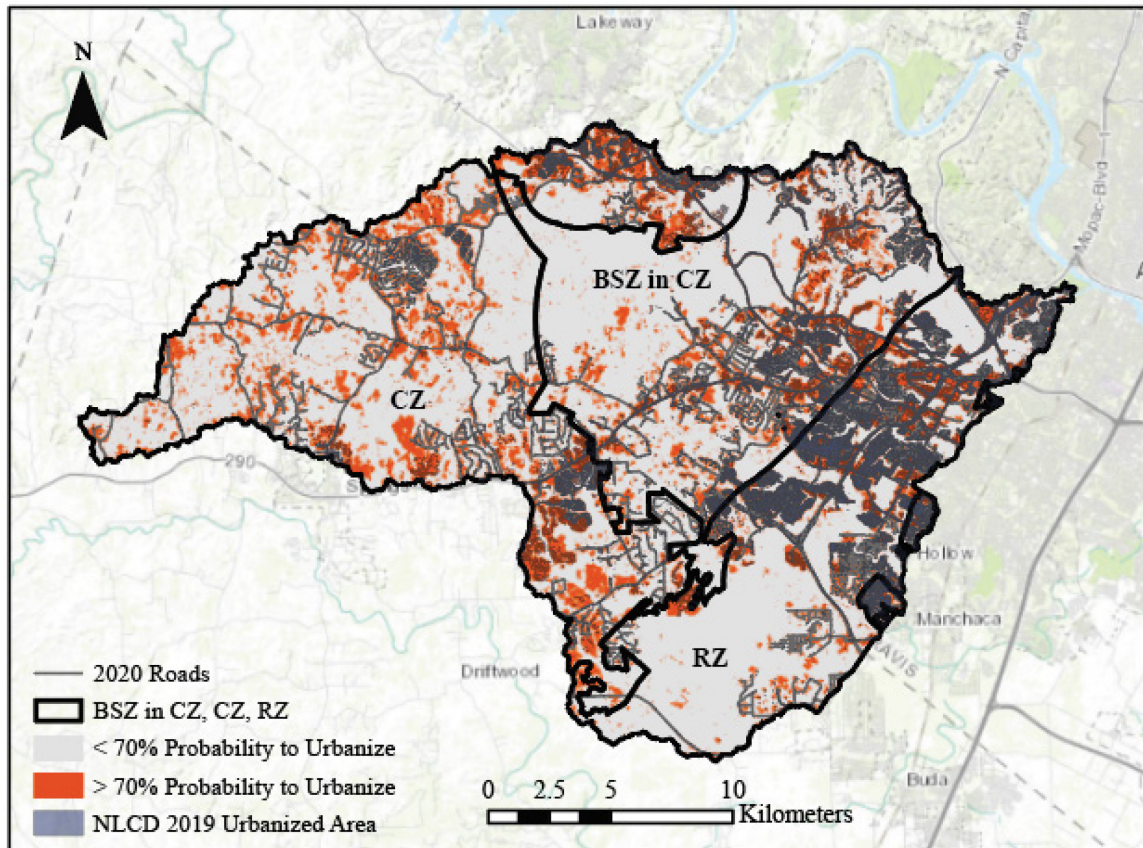


Figure 8. Urbanization as of 2042 as predicted by SLEUTH, urbanization as of 2019 in the NLCD 2019 LULC data, and the 2020 roads input layer for the aggressive scenario.

4.4 SWB Model Results

4.4.1 Current Mean Annual Recharge

For comparison, the final SWB calibration result is presented in Figure 9. This represents current mean annual recharge based on urbanized area in the NLCD 2019 LULC data. The mean annual recharge for the entire study area as modeled by SWB is equal to 13.13 cm. In the portion of the BSZ lying within the CZ, mean annual recharge is equal to 12.95 cm. In the CZ, mean annual recharge is equal to 13.28 cm, while in the RZ, mean annual recharge is equal to 13.06 cm. The results of all scenarios modeled by

SWB are within expectations regarding the relative amounts of mean annual recharge between scenarios based on the amount of impervious cover present in each zone. Table 7 summarizes mean annual recharge calculations for all SWB model scenarios. Table 8 summarizes the percent change in mean annual recharge between each scenario output and the current mean annual recharge. Figures showing SWB outputs are visualized using the Jenks method of natural breaks.

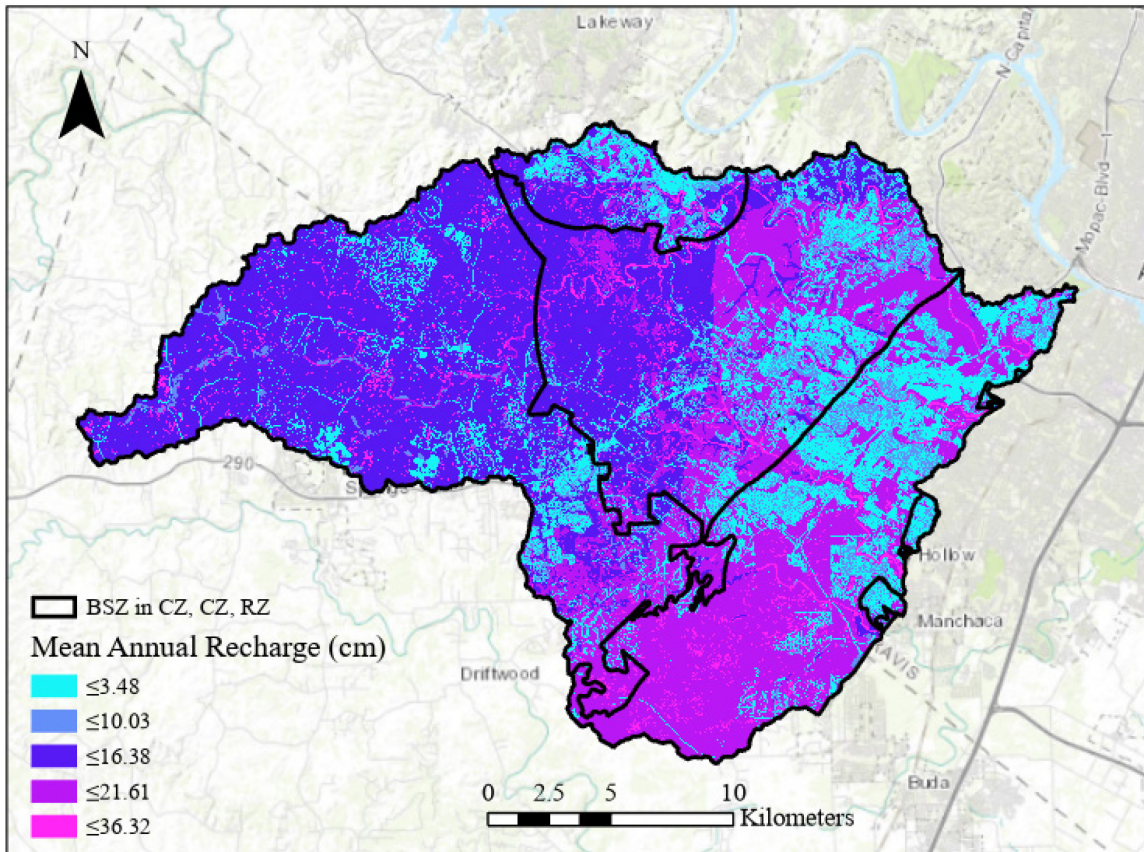


Figure 9. Current mean annual recharge as modeled by SWB.

Table 7. Summary of current mean annual recharge based on NLCD 2019 LULC data, and mean annual recharge based on SLEUTH scenarios as modeled by SWB.

Summary of Mean Annual Recharge by Zone (cm)				
Scenario	Study Area	BSZ in CZ	CZ	RZ
Current	13.13	12.95	13.28	13.06
Baseline	9.58	10.11	8.48	10.64
Extreme	8.38	9.19	6.91	9.73
Conservative	8.99	9.63	7.70	10.26
Aggressive	10.82	11.18	10.11	11.51

Table 8. Summary of the percent change in mean annual recharge between each SWB scenario output and the current mean annual recharge based on NLCD 2019 LULC data.

Summary of % Change in Mean Annual Recharge by Zone				
Scenario	Study Area	BSZ in CZ	CZ	RZ
Current	-	-	-	-
Baseline	-27%	-22%	-36%	-18%
Extreme	-36%	-29%	-48%	-25%
Conservative	-32%	-26%	-42%	-21%
Aggressive	-18%	-14%	-24%	-12%

4.4.2 Baseline Scenario

The baseline scenario was simulated by reclassifying cells in the NLCD 2019 LULC data that were predicted to urbanize in the baseline scenario derived by SLEUTH as “Developed – Medium Intensity”. It represents mean annual recharge by 2042 if no action is taken by the COA to alter limits to impervious cover within the study area. The resulting mean annual recharge predicted by the model is presented in Figure 10. The total amount of recharge predicted by the model in this scenario is equal to 9.58 cm. In the portion of the BSZ lying within the CZ, the amount of recharge is equal to 10.11 cm. In the CZ, the amount of recharge is equal to 8.48 cm, while in the RZ, the amount of recharge is equal to 10.64 cm.

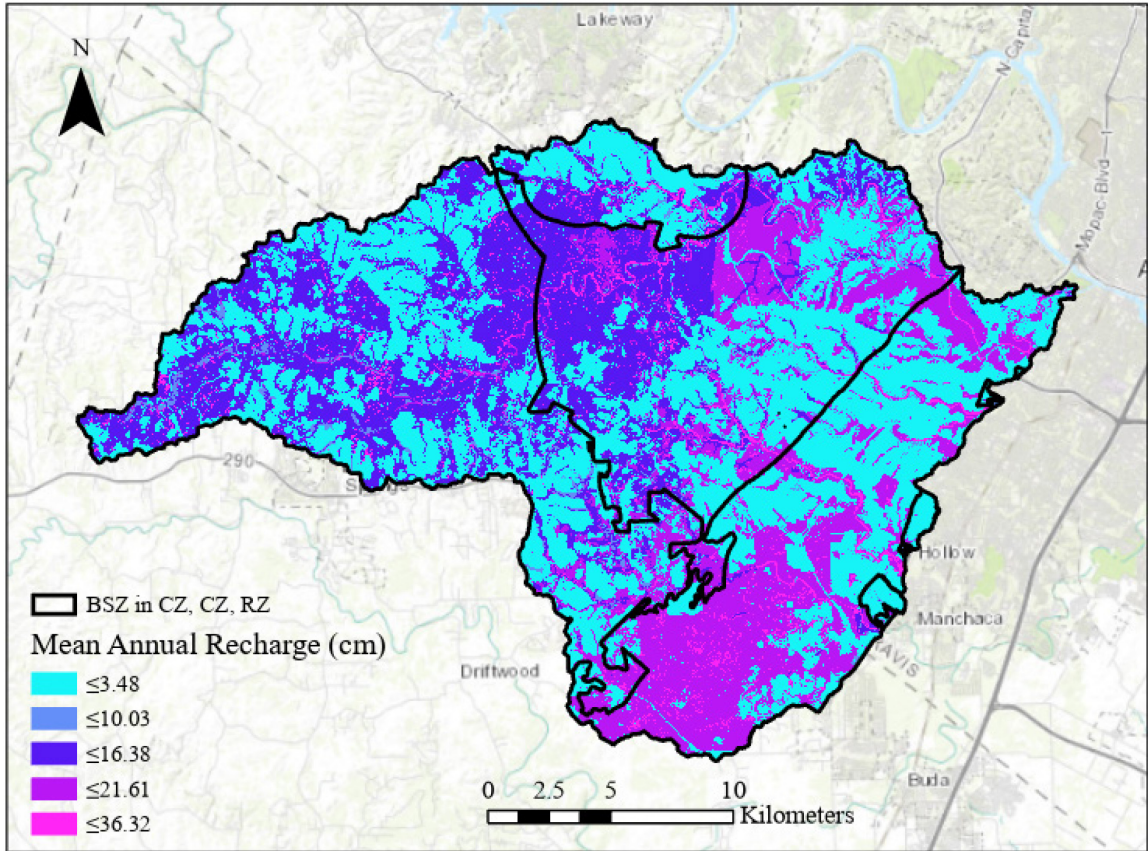


Figure 10. Mean annual recharge for the baseline scenario as predicted by SWB.

4.4.3 Extreme Scenario

The extreme scenario was simulated by reclassifying cells in the NLCD 2019 LULC data that were predicted to urbanize in the extreme scenario derived by SLEUTH as “Developed – Medium Intensity”. It represents possible impacts to aquifer recharge if extreme urban growth through 2042 is allowed to take place. The resulting mean annual recharge predicted by the model is presented in Figure 11. The total amount of recharge predicted by the model in this scenario is equal to 8.38 cm. In the portion of the BSZ lying within the CZ, the amount of recharge is equal to 9.19 cm. In the CZ, the amount of recharge is equal to 6.91 cm, while in the RZ, the amount of recharge is equal to 9.73 cm.

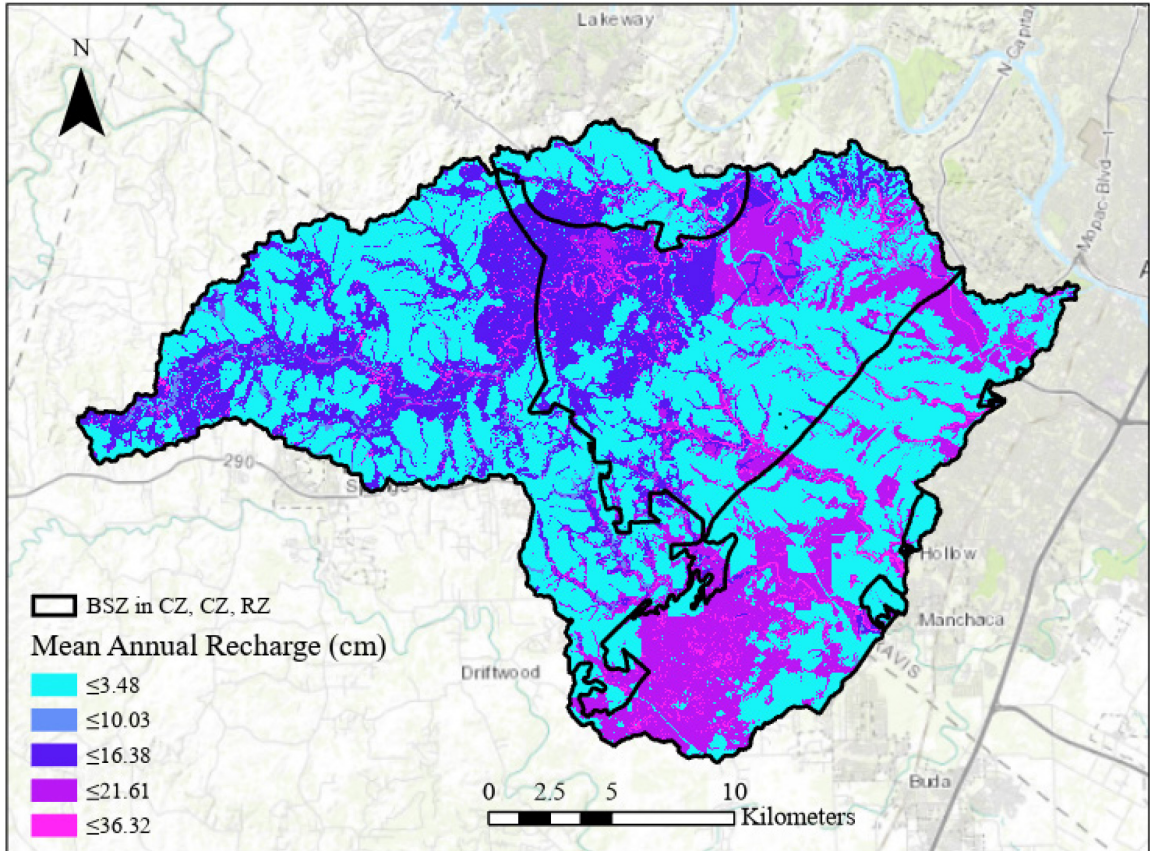


Figure 11. Mean annual recharge for the extreme scenario as predicted by SWB.

4.4.4 Conservative Scenario

The conservative scenario was simulated by reclassifying cells in the NLCD 2019 LULC data that were predicted to urbanize in the conservative scenario derived by SLEUTH as “Developed – Medium Intensity”. It represents possible impacts to aquifer recharge by 2042 if the COA applied a 5% reduction in restriction to impervious cover in each zone, therefore allowing for 20% impervious cover limit in the RZ, 25% impervious cover limit in the BSZ within the CZ, and 30% impervious cover limit in the CZ. The resulting mean annual recharge predicted by the model is presented in Figure 12. The total amount of recharge predicted by the model in this scenario is equal to 8.99 cm. In the portion of the BSZ lying within the CZ, the amount of recharge is equal to 9.63 cm. In the CZ, the amount of recharge is equal to 7.70 cm, while in the RZ, the amount of

recharge is equal to 10.26 cm.

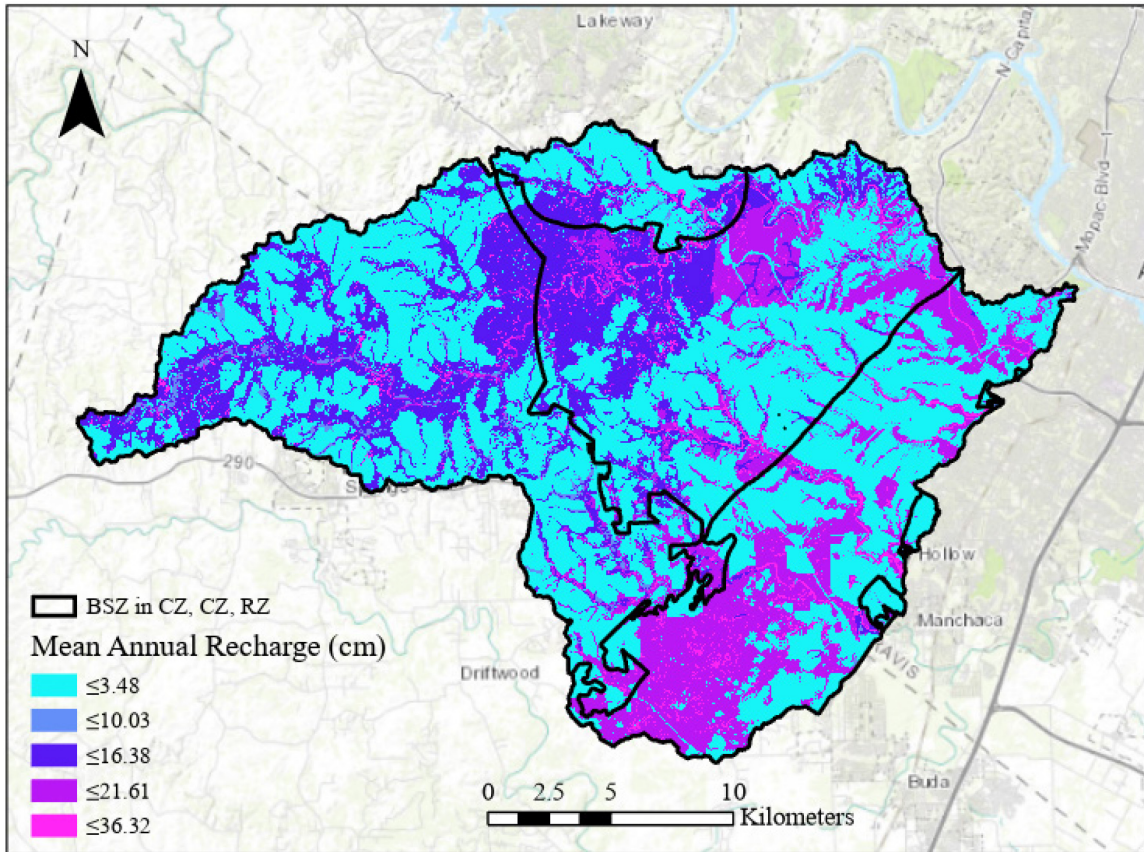


Figure 12. Mean annual recharge for the conservative scenario as predicted by SWB.

4.4.5 Aggressive Scenario

The aggressive scenario was simulated by reclassifying cells in the NLCD 2019 LULC data that were predicted to urbanize in the aggressive scenario derived by SLEUTH as “Developed – Medium Intensity”. It represents possible impacts to aquifer recharge by 2042 if the COA applied a 5% increase in restriction to impervious cover in each zone, therefore allowing for 10% impervious cover limit in the RZ, 15% impervious cover limit in the BSZ within the CZ, and 20% impervious cover limit in the CZ. The resulting mean annual recharge predicted by the model is presented in Figure 13. The total amount of recharge predicted by the model in this scenario is equal to 10.82 cm. In the portion of the BSZ lying within the CZ, the amount of recharge is equal to 11.18 cm.

In the CZ, the amount of recharge is equal to 10.11 cm, while in the RZ, the amount of recharge is equal to 11.51 cm.

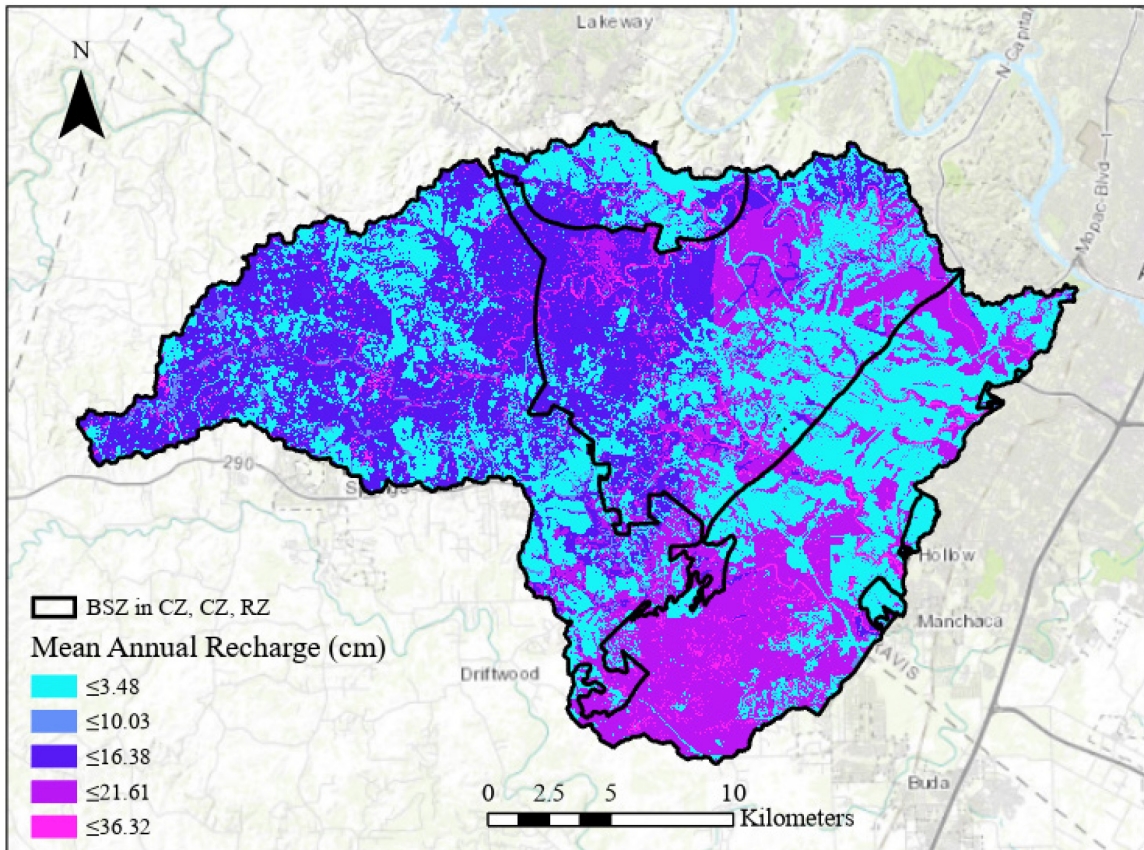


Figure 13. Mean annual recharge for the aggressive scenario as predicted by SWB.

4.5 Hypothesis Testing

Each cell from the baseline SWB output was compared against corresponding cells in the extreme, conservative, and aggressive scenarios using the `rstatix` package in R to test for significant difference in mean annual recharge values using an alpha value of 0.05. Results show that all three scenarios are significantly different from the baseline scenario, requiring a rejection of the null hypothesis. Thus, there is a significant difference in recharge rate among the zones and scenarios within the study area.

The same cells were used in the Kruskal-Wallis test to examine the independent distribution of recharge values in each zone, and to compare zones across scenarios using the rstatix package using an alpha value of 0.05. Results show that in each case, the distribution of recharge values is significantly different than others, changes to impervious cover do cause a significant difference in the amount of recharge received by the aquifer, in terms of both the respective limits applied to each zone and the general limits applied in each scenario, as zones within each scenario were found to differ, as well as zones across scenarios. Mean annual recharge as a function of area urbanized by SLEUTH for each zone in each scenario is presented in Figure 14. Boxplots showing the range, minimum, maximum, and median values for SWB scenario outputs are presented in Figure 15.

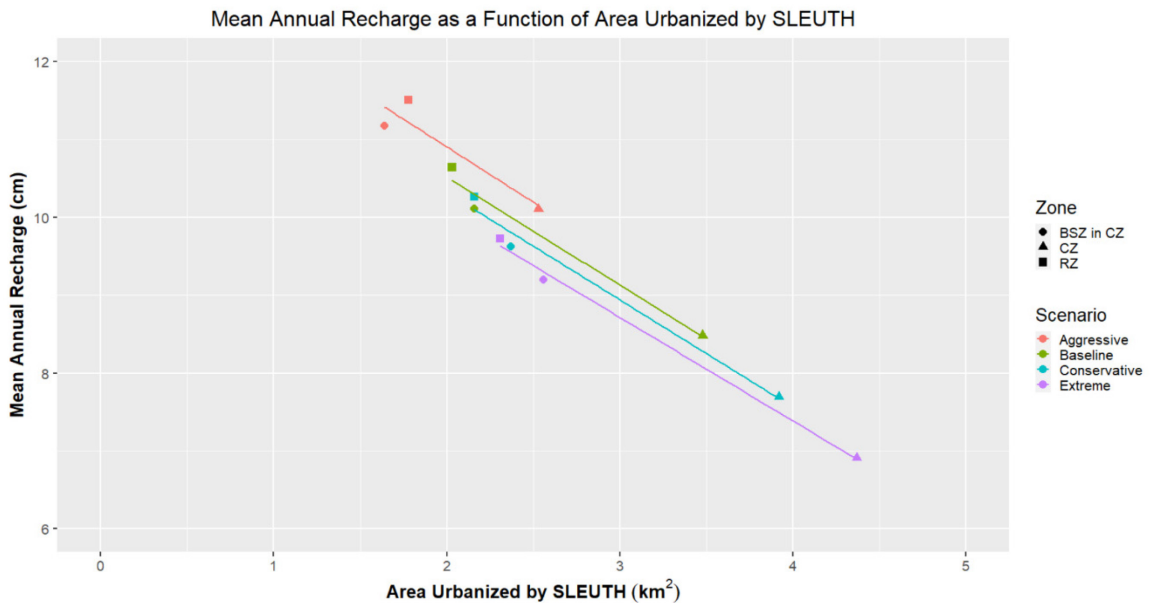


Figure 14. Scatterplot showing mean annual recharge as a function of area urbanized by SLEUTH for each zone in each scenario.

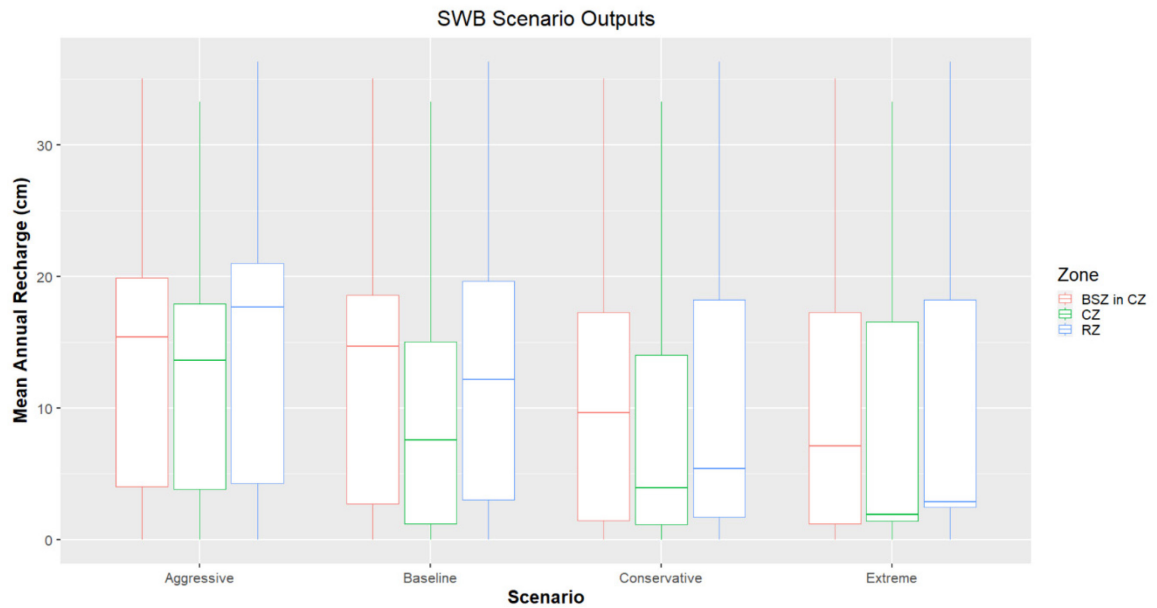


Figure 15. Boxplots showing the range, minimum, maximum, and mean values of each zone as predicted by SWB for the baseline scenario.

5.0 DISCUSSION

5.1 SLEUTH Calibration

The “Urban” class used by the MLC algorithm for identifying pixels of built-up area is an umbrella term that represents a broad class that contains a mix of different land cover. Although care was taken to provide the MLC with accurate representations of the various materials used to construct buildings and other features synonymous with urban areas, it is likely that the algorithm mislabeled land-cover types that should be considered urban but don’t include these materials as “non-Urban”. Therefore, the urban extents used in SLEUTH calibration may not be as accurate as those that might have been produced by a more granular classification scheme.

The BFC derived in SLEUTH calibration represent the type of growth that the study area has experienced since 2005. The high Road Gravity parameter observed in Table 3 can be interpreted to mean that urban growth here has a high affinity for major roadways, as they carried the most weight in the transportation input. There also exists a moderately high amount of urban sprawl based on the Breed, Diffusion, and Spread parameters. Breed represents the establishment of new urban centers. The high Breed parameter (72) derived in calibration means that disconnected satellite communities commonly form in the study area, often connected to more densely populated areas like central Austin by major roadways. The areas north of State Highway 290W that lie in and around Dripping Springs in the southern CZ, and the CZ perimeter in general, displayed this phenomenon most prominently. Others have found this combination of Road Gravity and Breed parameters to produce similar results (Dezhkam et al., 2013; Rafiee et al., 2009).

Diffusion represents spontaneous growth through the random urbanization of land. The relatively high Diffusion parameter (68) derived in calibration means that these disconnected satellites are often established in sprawling patterns as the antithesis of overall compact and efficient urban growth throughout the study area. This is often through the conversion of agricultural land to residential or low-intensity commercial. Yang and Lo (2003) calibrated to a Diffusion parameter of 71 and found that it led to this type of growth. In their study, satellite communities eventually grew together to form a new edge of the major Atlanta, GA metropolitan region. The Williamson Creek watershed near Oak Hill in the northern RZ and eastern BSZ in CZ is a noticeable example of this type of growth output by SLEUTH.

Spread simulates outward or inward edge growth, where newly urbanized centers expand, and plays a very important role regarding the kind of urban sprawl taking place. The relatively low Spread parameter found to exist in this study (42) means that although sprawling patterns do exist between satellite communities, each satellite resembles a tight cluster of infill growth, where grid-like systems of intermediate and minor roadways facilitate life. This often occurs in newly converted suburbs along the peri-urban fringe, such as those found within the study area. Mahiny and Clarke (2013) found that a Spread coefficient of 47 led to compact urban centers located along the periphery of existing development, which in their study, led to an increase in overall runoff volume throughout the study area. This presents a paradox for this study area, as compact growth is preferred, but if it remains disconnected to larger urban centers, impacts to hydrology are compounded. The relatively high Slope parameter (64) means that urban growth in and around satellite communities is greatly influenced by slope

degree, taking place in locations of relatively low topographic relief. This is a positive result in terms of the impact of urbanization upon the natural environment, as hillslopes naturally experience high rates of runoff.

The extremely high Diffusion, Breed, Spread, and Road Gravity parameters (82, 91, 81, and 86) of the extreme scenario indicate that the same underlying pattern of tight knit, but disconnected satellite communities may have existed even before the inception of the SOS Ordinance. This may be a function of urban planning dogmas taught at area universities in decades past, or of local or state urban growth policies. Given that Spread and Diffusion are much closer in parameter space here, those satellite communities quickly form the new edge of major metropolitan Austin in this scenario. The Slope parameter (68) remaining nearly equal between all scenarios suggests that the same mechanisms behind other parameters derived by this model have for some time taken the high topographic relief of central Texas into account, as building upon hillslopes is more expensive and causes more degradation to the environment through erosion.

5.2 SWB Calibration

Ideally, SWB is calibrated to a single stream gage located near the outlet of a single control watershed. However, due to widely varying landscape characteristics observed between study area watersheds, coupled with stream gages located far away from watershed outlets near the RZ boundary, this ideal calibration routine could not be implemented in this study. However, the calibration method used for SWB in this study has precedent in past literature (McCoy, 2016; Westenbroek, 2010).

The chosen configuration of stream gages used for calibration also had impacts upon the SWB model outputs, perhaps causing the model to underestimate the recharge

rate across the model domain. Gage 0815530 was used due to its location in the lower portion of the Barton watershed. However, the amount of recharge computed for this gage (Table 4) may not be an accurate reflection of the true amount of recharge taking place in the watershed due to Barton Creek possibly losing much flow to the aquifer as it passes over the RZ. Gage 08155240 may have provided a more accurate representation of recharge in the calibration phase, as it lies northwest of the RZ boundary.

Because the impervious cover limits imposed by the original SOS Ordinance vary by zone, and sprawling patterns of growth have caused major differences in their respective land-cover, the watersheds contributing to Barton Springs remain a difficult location for hydrologic modeling. Further analysis into calibration of aquifer recharge models in the study area may shed new light upon proper techniques for producing more accurate results.

5.3 SLEUTH Scenarios

The baseline scenario provided a relatively moderate amount of growth in all zones and seems to strike the best balance of all scenarios in regard to managing Austin's high growth rate with sustainable practices. Here, 86% of available land, or land not excluded from future growth by SLEUTH, was urbanized by the model, mainly in places of low slope angle, protecting the most vulnerable natural features – the hillslopes, from erosion. At a minimum, the original SOS Ordinance has been successful in managing development in a highly sensitive environmental zone with an optimal set of impervious cover limits. A 67% overall increase in urbanized area compared to the NLCD 2019 data over a twenty-year period in which Austin is poised to boom seems reasonable, and

suggests that the continuation of the 15 – 25% limit is deemed a good balance that meets both human and environmental needs (Table 6).

The extreme scenario demonstrated that if extensive urban growth is allowed to take place in the study area over this time, almost all land available to SLEUTH for development could become urbanized, as 97% of land not excluded from SLEUTH was converted in this scenario. The initial satellite communities form around major roadways early in the simulation before the high Spread and Diffusion parameters cause them to adjoin through infill and compact growth, where eventually, they dissolve into southwest-central Austin. This is observed most prominently in the Oak Hill and Slaughter Creek areas spanning portions of the BSZ in CZ, and RZ in Figure 6. This pattern may be positive for increasing connectivity and mobility for residents, and for reducing runoff volume, as there would exist less urban sprawl, but the resulting runoff could contain a high degree of pollutants due to the dense urbanization and construction along hillslopes.

The conservative scenario saw a conversion of 91% of land not excluded from SLEUTH urbanization, meaning that even a small decrease of 5% in impervious cover limits could have drastic consequences. This scenario saw the second highest increase over NLCD 2019 data in urbanized land in the sensitive RZ, and 195% increase in the CZ (Table 6). The early formation of satellites here lacks the eventual infill growth and connection with the Austin metro area, therefore exacerbating sprawl and runoff while decreasing recharge. This scenario is not ideal, and although it strikes a balance between society and the environment, the scales may be easily tipped in a negative direction if care is not taken on a micro level to control exactly where growth takes place.

The aggressive scenario is by far the most sustainable outcome in terms of minimizing degradation to the environment. Here, only 78% of land available to urbanization by SLEUTH is converted, and only 9% of that takes place in the two most sensitive zones – the BSZ in CZ and RZ. Although there is a 90% increase in area urbanized in this scenario, it takes place mostly in Little Barton and Bear watersheds, far away from Barton Springs and the RZ, as well as Barton Creek. However, this scenario is not likely given the wide expanse of land available to SLEUTH for development throughout much of the CZ, nor is it in balance with Austin’s need to house the in-migrants expected to arrive over the next two decades.

Based on NLCD 2019 data, the amount of current urbanized area located in the RZ (1.71 km²) is greater than that found in the CZ (1.33 km²) and BSZ in CZ (1.56) (Table 5). This pattern does not continue throughout the SLEUTH scenarios, except for the aggressive, where impervious cover in the RZ was held to a 10% limit. This is observed in current data because the RZ is closer to Austin’s city center and contains a denser road network, where neighborhoods built in the early- to mid-20th century near Barton Springs are located. This means that growth before SOS enactment was taking place at a high rate in the RZ, when knowledge about the Edwards Aquifer was just beginning to emerge. A possible reason why the aggressive scenario output by SLEUTH displays this pattern is that limits to other zones in this scenario were severe enough that new development there was not able to outpace the old growth that exists currently. Overall, the RZ showed the least growth compared to others, despite having the most initial urbanized area. This is taken to be directly related to the lower impervious cover limits imposed there and is a sign that protecting recharge to the

Edwards Aquifer begins by limiting growth in the RZ. The COA has achieved this goal by purchasing water quality protection lands in the extreme southern portion of the RZ. The zone also had the least amount of total area (141 km²), and the highest amount of land excluded from development by SLEUTH (98 km²).

The CZ saw the most growth in each of the SLEUTH scenarios, with a near 200% increase in area urbanized in the baseline, extreme, and conservative scenarios, and a near 100% increase in the aggressive. Its location along the existing peri-urban fringe offers space for development of the disconnected, sprawling satellite communities shown to take place by the SLEUTH parameters. The model's affinity for major roadways caused major growth to develop north of Highway 290W in the southern portion of the zone, and infill growth of satellites caused by the relatively low Spread parameter ensured dense development in the communities that formed. It also contained the most undeveloped land for the model to urbanize – 225 km² total, with only 36% of the zone being excluded from SLEUTH development, compared to 63% in the BSZ in CZ, and 69% in the RZ. There are policy implications at play in this zone as well, as most of the zone lies in Hays County, where there exists less land excluded from development by the SLEUTH model.

The BSZ in CZ saw an intermediate amount of growth predicted by SLEUTH. Although this zone contained a slightly smaller portion of excluded area than the RZ, and more total area (168 km²), growth here was limited by the Slope parameter in SLEUTH. The zone contains the highest average slope at 4.61°, compared to 3.64° in the CZ and 2.42° in the RZ. Development in this zone is expensive and difficult due to the Hill Country setting and likely more degradational to erosion on hillslopes and to water

quality in lower waterways like Barton Springs. High slope angles also mean less area available for development due to NSA calculations on a site-by-site basis. It is the portion of the study area where precipitation directly recharges the Springs, therefore obtaining building permits in this zone is more difficult than in the CZ, and it contains more dendritic waterways than other zones, thus more WQTZ and CWQZ riparian buffers, as the headwaters of Williamson, Slaughter, and Bear Creeks originate here.

5.4 SWB Scenarios

Currently, aquifer recharge within the study area is highest in the extreme southern portion of the RZ. This pattern persists throughout all SWB scenarios, likely due to a large swath of water quality protection lands excluded from development northwest of Buda and a low average hillslope angle. Soil group A showed the highest amount of recharge throughout the SWB model domain, as it carries the highest infiltration capacity and is made up of mostly alluvial beds in and around creeks. This places even more importance on the current WQTZ and CWQZ riparian buffers to maintain healthy ecosystems near waterways, and to protect against pollutants reaching the alluvial creek beds where they may easily infiltrate the RZ. The RZ currently shows a higher density of urbanization than other zones, and low recharge rates tend to penetrate these buffers in areas of dense urbanization, encroaching upon the creeks. The current recharge scenario highlights the importance of current SOS limits in minimizing negative impacts to the aquifer in the RZ.

Current recharge is mostly uniform across the CZ, especially in the upper portions of the Barton watershed where shrubland and deciduous forest dominate the landscape and there currently exists a notable lack in urban development (Figure 9). Toward the

lower portion of the zone in Bear watershed, recharge rates begin to increase dramatically due to the extremely high patch of recharge in and around the RZ water quality protection lands. This again highlights the importance of action by the COA in protecting the aquifer, as the CZ will eventually see the most urbanization as modeled by SLEUTH.

Most notable in the BSZ in CZ is an abrupt change in recharge rate that bisects the zone south from the lower portions of Bear watershed in the CZ, north to the upper portion of the BSZ in CZ (Figure 9). This abrupt pattern does not appear in any SELTUH outputs, nor does it appear in the SWB inputs. However, upon further inspection, this line follows in a general fashion where the dendritic patterns forming the headwaters of Williamson, Slaughter, and Bear Creeks exist, and is where overland flow running southeast from the CZ towards the RZ begins to encounter alluvial beds that facilitate higher recharge (Figure 9). This abrupt change in recharge rate is observed in all SWB outputs, with slight variation in the east-west boundary between them, and currently contains a dense patch of urban development (Figures 10 – 13). This, again, highlights the importance of SOS riparian buffers and impervious cover limits in keeping the low Spread parameter in SLEUTH from infilling this area to maintain current recharge rates.

The baseline SWB scenario (Figure 10) saw a decrease of 3.55 cm in mean annual recharge across the study area, leaving 2042 recharge at 73% of its current rate. The biggest contributing factor to this decrease is the 67% increase in urban area found by SLEUTH (Figure 5). In this scenario, as well as others, the dramatic impact of urbanization is observed in the sharp declines in recharge where SLEUTH predicted land to develop. In the CZ, the riparian buffer around Barton Creek seems the only barrier to

the convergence of development along the northern edge of the watershed with that stemming from the south along Highway 290W. This zone is critical for achieving sustainable development through 2042, as it contains the most wilderness of all zones at the simulation's outset and saw the largest increases in urbanized area and the largest decreases in recharge. Compared to other scenarios, the baseline again seems to strike the best balance between Austin's need for growth and care for the environment, meaning the SOS limits to impervious cover should not be altered.

The extreme scenario (Figure 11) saw a 36% decrease in mean annual recharge across the study area brought on by the 101% increase in urban area predicted by SLEUTH (Figure 6). Here, almost the entire southern portion of the CZ sees a sharp decrease in recharge. This is alarming as the water quality protection lands lie just southeast of this area in the RZ. Because of the close proximity of this dramatic decrease in recharge to the RZ boundary, overland flow running southeast would have a very short distance to travel before reaching the protected lands and infiltrating the aquifer. In the BSZ in CZ, the area near the headwaters of Williamson, Slaughter and Bear creeks become inundated with low recharge values in the extreme SWB scenario due to the infill of satellite development brought on by the SLEUTH Spread parameter. Without limits to impervious cover here, the creeks may become choked with eroded material carried by runoff, thus increasing the probability of flash floods in a now densely populated area.

The conservative scenario output by SWB (Figure 12) does not differ much from the extreme, with only a 4% difference in change to annual mean recharge separating the two (Figure 15). This means that even a decrease of 5% to current SOS limits could have drastic consequences to local hydrology. Many of the same issues that arise with the

extreme scenario plague this one as well. A 42% decrease in recharge in the CZ would likely form direct runoff to the RZ and exacerbate flash flooding. The 21% decrease in recharge to the RZ could compound with future drought, lowering the water table and decreasing fresh water supply.

The aggressive scenario (Figure 13) had the least impact upon aquifer recharge, but again seems unlikely to be implemented by the COA, as the 27% decrease in mean annual recharge produced by current SOS limits compares well to the 18% decrease observed in this scenario (Figure 10). The aggressive scenario would protect the RZ boundary, as well as the forested uplands of the CZ and headwater areas of the BSZ in CZ, but the reality of Austin's population boom and the economic windfall that will follow are powerful incentives for the COA to keep current SOS limits in place.

5.5 Hypothesis Testing

Significant differences in mean annual recharge found among zones and scenarios imply that the amount of aquifer recharge observed throughout the study area is directly attributable to the amount of impervious cover present. This directly addresses the research question and highlights the importance of the original SOS Ordinance in protecting the quantity and quality of recharge entering the Edwards Aquifer. Results of the statistical tests show that if any alteration is made to the ordinance in future scenarios, significant impacts to aquifer recharge will take place. In the case of the aggressive scenario, where limits to impervious cover are increased, these impacts are positive, as more recharge will reach the aquifer compared to the baseline, extreme, and conservative scenarios. In the case of the extreme and conservative scenarios, where extensive growth takes place or impervious cover limits are decreased, the impacts will be negative, as less

recharge will reach the aquifer compared to the baseline and aggressive scenarios. In light of the recent approval of the 45SW toll road in the southern RZ, this implies that the Edwards Aquifer may see increased vulnerability, as the major road is sure to bring development to areas currently excluded from urbanization by SLEUTH in this study.

The main effect of impervious cover limits on aquifer recharge is similar in direction across scenarios, as there is a significant negative relationship between aquifer recharge and amount of impervious cover limit imposed (Figure 14). However, there does seem to be a slight interaction effect of impervious cover on the magnitude of recharge in the aggressive and extreme scenarios (Figure 15). Recharge in the aggressive scenario did not take on the same relative pattern as other scenarios, as the RZ is predicted to be highest, compared to second highest in others. Recharge in the extreme scenario was found to be impacted at a much higher magnitude, especially in the CZ and RZ. This may be due to the extreme difference in amount of area urbanized in each scenario (Table 5). It is noteworthy that other possible independent variables may be at play that might cause this interaction. For instance, recharge is a function of terrain slope. Although flow direction was considered in the SWB model, slope angle between cells was not. Additionally, to a large degree, urban growth is a function of population density and average household income. Household size nor income were considered in the SLEUTH model.

5.6 Limitations

Because SLEUTH has no direct implementation for setting limits to urban growth, the results present an approximation of urban area in 2042. The amount of area urbanized by the model in each scenario, and the subsequent impacts to aquifer recharge

predicted by SWB, should be taken as an imprecise estimation of what the future may hold for growth in the study area and how that growth may impact the Edwards Aquifer. It remains difficult to precisely portray a given policy in a scientific model, as technical limitations exist between real world systems and what computer systems are capable of computing.

Due to SLEUTH's inability to distinguish the degree of urbanization in a given cell, the assignment of 'Developed - Medium Intensity' to newly urbanized cells in the SWB LULC input layer represents a large source of uncertainty in this model and is perhaps an overgeneralization of the type of growth that will take place. However, this is the most appropriate action, as speculation about the intensity of newly urbanized cells would be arbitrary and detrimental to the overall accuracy of the recharge model. SLEUTH is also incapable of simulating vertical growth, and a proxy for this type of growth could not be found when building model input layers. This means that population density, and the impacts that may have on increasing the amount of area developed as time goes on, is not represented by the model. Only horizontal growth is depicted. Perhaps if vertical growth had been incorporated into the model, recharge rates across the model domain may have decreased even more, as a positive feedback loop may exist between population density and amount of impervious cover needed to support it.

The 30 m spatial resolution of Landsat imagery that was used to project future urban extents is relatively coarse by modern day standards, but a lack of funding for access to proprietary imagery produced by private companies dictates that Landsat data be used. This spatial resolution is common throughout SLEUTH literature, and although details were undoubtedly lost in pixels of mixed land-use, the model produced enough

detail to make sound conclusions about impacts to aquifer recharge. Uncertainty in land-use type and degree of impervious cover associated with each were approximated in the LU lookup table used for input to SWB. Care was taken to follow convention in building this table, as construction materials and associated runoff curve numbers do not vary widely.

6.0 CONCLUSION

If Austin is to remain at its current pace of growth, the SOS Ordinance must either be left intact or reinforced through more strict limitations to impervious cover. The baseline scenario suggests that the study area will likely experience at least a 3.55 cm decrease in mean annual recharge given the current rate of urban growth over the next twenty years. If the conservative or extreme scenarios are allowed to take place, the study area may experience a decrease of 4.14 cm – 4.75 cm. Given that the best-case scenario – the aggressive, will likely lead to a decrease of only 2.31 cm, prompt effort in ensuring that the current SOS Ordinance remains intact is of high importance and makes a significant impact on the future of our natural resources. This highlights the power and practical significance of the work presented in this study. Decision makers at all levels of government and industry need sound scientific information regarding future forecasts of the impacts of societal progression on the natural world. Compounded with other negative impacts from global climate change, the absence of studies such as that presented here could spell disaster for an already vulnerable landscape and human population by further degrading water quality in the Edwards and leaving future populations more prone to water shortages and degradation to water quality.

Based on the findings of this research, it may be valuable for future research to explore the impacts of impervious cover upon aquifer recharge using a more robust urban growth model, such as an agent-based model, or proprietary software. Linking outputs to SWB and comparing to those produced by this study may provide new knowledge in both the urban modeling sphere, as well as the hydrologic, as the uncertainties of SLEUTH may become more readily apparent, and strengths of SWB may be better leveraged. An

additional independent variable in the SLEUTH-SWB paradigm may provide a next-step as well. Knowing the influence of political partisanship, income, or education on urban growth and the subsequent impacts to aquifer recharge may provide interesting insights beyond those discussed here. Finally, representing population density through vertical growth remains a difficult but worthy endeavor for future researchers. This variable may provide more certainty to the urban growth model and could lead to more accurate predictions of impacts to aquifer recharge.

REFERENCES

- Abraham, M., Ann Mathew, R., & Jayapriya, J. (2021). Numerical Modeling as an Effective tool for Artificial Groundwater Recharge Assessment. *Journal Of Physics: Conference Series*, 1770(1), 012097. <https://doi.org/10.1088/1742-6596/1770/1/012097>.
- Ainiwaer, M., Ding, J., Wang, J., & Nasierding, N. (2019). Spatiotemporal Dynamics of Water Table Depth Associated with Changing Agricultural Land Use in an Arid Zone Oasis. *Water*, 11(4), 673. <https://doi.org/10.3390/w11040673>.
- Ali Rahmani, S., & Chibane, B. (2018). Delineation of potential recharge area using a hybrid model, case of Djelfa Hadjia watershed. *Arabian Journal Of Geosciences*, 11(9). <https://doi.org/10.1007/s12517-018-3573-8>.
- Alkhatib, J., Engelhardt, I., & Sauter, M. (2021). Identification of suitable sites for managed aquifer recharge under semi-arid conditions employing a combination of numerical and analytical techniques. *Environmental Earth Sciences*, 80(17). <https://doi.org/10.1007/s12665-021-09797-y>.
- Aminpour, P., Gray, S., Beck, M., Furman, K., Tsakiri, I., & Gittman, R. et al. (2022). Urbanized knowledge syndrome—erosion of diversity and systems thinking in urbanites' mental models. *Urban Sustainability*, 2(1). <https://doi.org/10.1038/s42949-022-00054-0>.
- Antolino, D. (2022). *Soil-Water-Balance (SWB) model datasets for the Greater Wake County area, North Carolina, 1981–2019*. Reston: U. S. Geological Survey.

- Austin Chamber of Commerce. (2022a). *Austin Migration Insights*. Austin: Austin Chamber of Commerce. Retrieved from <https://www.austinchamber.com/blog/02-08-2022-migration>.
- Austin Chamber of Commerce. (2022b). *Job Growth & Unemployment*. Austin: Austin Chamber of Commerce. Retrieved from <https://www.austinchamber.com/blog/06-21-2022-job-growth-unemployment>.
- Aquifer Alliance*. Aquifer Alliance | Protection and preserve the Edwards Aquifer. (2022). Retrieved from <https://aquiferalliance.org/>
- Ayazli, I. (2020). Using the Total Exploratory Factor Analysis (T-EFA) as a Calibration Technique for SLEUTH Model. *The International Archives of The Photogrammetry, Remote Sensing and Spatial Information Sciences, XLIV-4/W3-2020*, 85-88. <https://doi.org/10.5194/isprs-archives-xliv-4-w3-2020-85-2020>.
- Bao, C., & He, D. (2019). Scenario Modeling of Urbanization Development and Water Scarcity Based on System Dynamics: A Case Study of Beijing–Tianjin–Hebei Urban Agglomeration, China. *International Journal of Environmental Research and Public Health*, *16*(20), 3834. <https://doi.org/10.3390/ijerph16203834>.
- Bassman, L. (2019). *Barton Creek to expand*. Statesman.com. Retrieved 26 July 2022, from <https://www.statesman.com/story/news/local/westlake/2019/06/20/developer-to-expand-barton-creek-neighborhood/4869689007/>.
- Batty, M. (2011). When all the world's a city. *Environment And Planning*, *43*(4), 765-772.

- Beddows, C. (2016). *What is Groundwater Modelling and Why is it Important?*
Scitechconnect.elsevier.com. Retrieved 30 July 2022, from
[https://scitechconnect.elsevier.com/what-is-groundwater-modelling-why-
important/](https://scitechconnect.elsevier.com/what-is-groundwater-modelling-why-important/).
- Benavidez, A. (2021). *The approval of a subject property that is set to be developed into an apartment complex had to be postponed by the Austin Zoning and Platting Commission last week due to the severe weather.* VirtualBX.com. Retrieved 26 July 2022, from <https://www.virtualbx.com/construction-preview/austin-local-real-estate-agency-to-build-apartment-development-on-35-7-acres/>.
- Bergström, S., & Lindström, G. (2015). Interpretation of runoff processes in hydrological modelling-experience from the HBV approach. *Hydrological Processes*, 29(16), 3535-3545. <https://doi.org/10.1002/hyp.10510>.
- Bihanta, N., Soffianian, A., Fakheran, S., & Gholamalifard, M. (2014). Using the SLEUTH Urban Growth Model to Simulate Future Urban Expansion of the Isfahan Metropolitan Area, Iran. *Journal of the Indian Society of Remote Sensing*, 43(2), 407-414. <https://doi.org/10.1007/s12524-014-0402-8>.
- Brabec, E. (2009). Imperviousness and Land-Use Policy: Toward an Effective Approach to Watershed Planning. *Journal Of Hydrologic Engineering*, 14(4), 425-433. [https://doi.org/10.1061/\(asce\)1084-0699\(2009\)14:4\(425\)](https://doi.org/10.1061/(asce)1084-0699(2009)14:4(425)).
- Bureau of Economic Geology. (2021). *Geologic Wonders of Texas*. University of Texas. Retrieved from <https://www.beg.utexas.edu/geowonders/centtex>.

- CAPCOG. (2021). *Comprehensive Economic Development Strategy* (p. 3). Austin, TX: Capital Area Council of Governments. Retrieved from <https://www.capcog.org/wp-content/uploads/2021/11/CEDS-2020-2025-Updated-Final.pdf>.
- Chaudhuri, G., & Clarke, K. (2019). Modeling an Indian megalopolis– A case study on adapting SLEUTH urban growth model. *Computers, Environment And Urban Systems*, 77, 101358. <https://doi.org/10.1016/j.compenvurbsys.2019.101358>.
- Chu, T., Yang, Y., Lu, Y., Du, X., & Ye, X. (2019). Clogging process by suspended solids during groundwater artificial recharge: Evidence from lab simulations and numerical modelling. *Hydrological Processes*, 33(25), 3226-3235. <https://doi.org/10.1002/hyp.13553>.
- Churkina, G. (2016). The Role of Urbanization in the Global Carbon Cycle. *Frontiers In Ecology and Evolution*, 3. <https://doi.org/10.3389/fevo.2015.00144>.
- City of Austin. (2022a). *Code of Ordinances*. Austin: City of Austin. Retrieved from https://library.municode.com/tx/austin/codes/code_of_ordinances?nodeId=TIT30AUTRCOSURE_CH30-5EN_SUBCHAPTER_AWAQU_ART13SAOUSPIN_S30-5-514POPRRE.
- City of Austin. (2022b). *Environmental Criteria Manual*. Austin: City of Austin. Retrieved from https://library.municode.com/tx/austin/codes/environmental_criteria_manual?nodeId=S1WAQUMA_1.5.0STBU.
- City of Austin. (2022c). *Environmental Criteria Manual, Appendix Q-1*. Austin: City of Austin. Retrieved from https://library.municode.com/tx/austin/codes/environmental_criteria_manual?nodeId=APXQ-1NESIAR.

- Clark, S., Harper, S., & Weber, B. (2022). *Growing Up in Rural America*. RSF: The Russell Sage Foundation Journal of The Social Sciences, 8(3), 1-47.
<https://doi.org/10.7758/rsf.2022.8.3.01>.
- Clarke, K., Brass, J., & Riggan, P. (1995). A cellular automaton model of wildfire propagation and extinction. *Photogrammetric Engineering And Remote Sensing*, 60(11), 1355 - 1367.
- Clarke, K., Hoppen, S., & Gaydos, L. (1996). Methods and Techniques for Rigorous Calibration of a Cellular Automaton Model of Urban Growth. In *Third International Conference/Workshop on Integrating GIS and Environmental Modeling*. Santa Fe; National Center for Geographic Information and Analysis. Retrieved 31 July 2022, from <https://pubs.er.usgs.gov/publication/70202456>.
- Clarke, K., Hoppen, S., & Gaydos, L. (1997). A self-modifying cellular automaton model of historical urbanization in the San Francisco Bay area. *Environment And Planning B: Planning And Design*, 24(2), 247-261.
<https://doi.org/10.1068/b240247>.
- Clarke, K., & Gaydos, L. (1998). Loose coupling a cellular automaton model and GIS: long-term urban growth prediction for San Francisco and Washington/Baltimore. *International Journal Of Geographical Information Science*, 12(7), 699-714. <https://doi.org/10.1080/136588198241617>.
- Corson-Dosch, N., & Garcia, C. (2022). *Soil-Water-Balance (SWB) model archive used to simulate annual upland recharge from infiltration of precipitation and snowmelt in the Harney Basin, Oregon, 1982-2016*. Reston: U.S. Geological Survey.

- Dams, J., Woldeamlak, S., & Batelaan, O. (2008). Predicting land-use change and its impact on the groundwater system of the Kleine Nete catchment, Belgium. *Hydrology And Earth System Sciences*, 12(6), 1369-1385. <https://doi.org/10.5194/hess-12-1369-2008>.
- Demographia. (2022). *DEMOGRAPHIA WORLD URBAN AREAS (Built Up Urban Areas or World Agglomerations)* (p. 3). St. Louis: Demographia. Retrieved from <http://www.demographia.com/db-worldua.pdf>.
- Dezhkam, S., Amiri, B., Darvishsefat, A., & Sakieh, Y. (2013). Simulating the urban growth dimensions and scenario prediction through sleuth model: a case study of Rasht County, Guilan, Iran. *Geojournal*, 79(5), 591-604. <https://doi.org/10.1007/s10708-013-9515-9>.
- Dietzel, C., & Clarke, K. (2004). Spatial Differences in Multi-Resolution Urban Automata Modeling. *Transactions In GIS*, 8(4), 479-492. <https://doi.org/10.1111/j.1467-9671.2004.00197.x>.
- Dietzel, C., & Clarke, K. (2007). Toward Optimal Calibration of the SLEUTH Land Use Change Model. *Transactions In GIS*, 11(1). <https://doi.org/10.1111/j.1467-9671.2007.01031.x>.
- Dri, G., Fontana, C., & Dambros, C. (2021). *Estimating the impacts of habitat loss induced by urbanization on bird local extinctions*. *Biological Conservation*, 256, 109064. <https://doi.org/10.1016/j.biocon.2021.109064>.
- Eichenbaum, J., & Gale, S. (1971). Form, Function, and Process: A Methodological Inquiry. *Economic Geography*, 47(4), 525. <https://doi.org/10.2307/142642>.

- Fry, M. (2011). From Crops to Concrete: Urbanization, Deagriculturalization, and Construction Material Mining in Central Mexico. *Annals of the Association of American Geographers*, 101(6), 1285-1306.
<https://doi.org/10.1080/00045608.2011.584289>
- Giardino, J., & Houser, C. (2015). *Principles and dynamics of the critical zone* (1st ed., p. 614). Elsevier.
- Ghimire, S., and J. Johnston. 2013. Impacts of domestic and agricultural rainwater harvesting systems on watershed hydrology: A case study in the Albemarle-Pamlico river basins (USA). *Ecohydrology & Hydrobiology* 13 (2):159-171.
- Gomes, L., F. Bianchi, I. Cardoso, R. Schulte, R. Fernandes, and E. Fernandes-Filho. 2021. Disentangling the historic and future impacts of land use changes and climate variability on the hydrology of a mountain region in Brazil. *Journal of Hydrology* 594:125650.
- Gómez, J., Guan, C., Tripathy, P., Duque, J., Passos, S., Keith, M., & Liu, J. (2021). Analyzing the Spatiotemporal Uncertainty in Urbanization Predictions. *Remote Sensing*, 13(3), 512. <https://doi.org/10.3390/rs13030512>.
- Goodarzi, M., Sakieh, Y., & Navardi, S. (2016). Scenario-based urban growth allocation in a rapidly developing area: a modeling approach for sustainability analysis of an urban-coastal coupled system. *Environment, Development and Sustainability*, 19(3), 1103-1126. <https://doi.org/10.1007/s10668-016-9784-9>.

- Greater Edwards Aquifer Alliance. (2021). *Edwards Aquifer Protection Plan* (p. 11).
Great Edwards Aquifer Alliance. Retrieved from
https://aquiferalliance.org/Library/LibraryFiles/Resources/Edwards_Aquifer_Protection_Plan.pdf.
- Guan, C., & Rowe, P. (2016). Should big cities grow? Scenario-based cellular automata urban growth modeling and policy applications. *Journal Of Urban Management*, 5(2), 65-78. <https://doi.org/10.1016/j.jum.2017.01.002>.
- Guerra, J., & Debbage, N. (2021). Changes in urban land use throughout the Edwards Aquifer: A comparative analysis of Austin, San Antonio, and the Interstate–35 corridor. *Applied Geography*, 133, 102480. <https://doi.org/10.1016/j.apgeog.2021.102480>.
- Hagerstrand, T., & Pred, A. (1967). *Innovation Diffusion as a Spatial Process*. Chicago: University of Chicago Press.
- Higgins, W. (2022). *Large housing development in the works on Barton Springs and Lamar - Austin Monitor*. AustinMonitor.com. Retrieved 26 July 2022, from <https://www.austinmonitor.com/stories/2022/06/large-housing-development-in-the-works-on-barton-springs-and-lamar/>.
- Hobby Center for Public Policy. (2014). *Projections of the Population of Texas and Counties in Texas by Age, Sex, and Race/Ethnicity from 2010 to 2050* (p. 9). Houston: University of Houston. Retrieved from https://uh.edu/hobby/_docs/research/population/2014%20PPRLE-SV2.pdf.

- Iowa Community Indicators Program. (2022). *Urban Percentage of the Population for States, Historical*. Ames: Iowa State University. Retrieved from <https://www.icip.iastate.edu/tables/population/urban-pct-states>.
- Jacobs, J. (1961). *The Death and Life of Great American Cities*. New York: Random House.
- Johnson, K. (2022). *Rural America Lost Population Over the Past Decade for the First Time in History*. University of New Hampshire - Carsey School of Public Policy. Retrieved from <https://carsey.unh.edu/publication-rural-america-lost-population-over-past-decade-for-first-time-in-history>.
- Kassogu , H., Bernoussi, A., Amharref, M., & Ouardouz, M. (2017a). Cellular automata approach for modelling climate change impact on water resources. *International Journal Of Parallel, Emergent And Distributed Systems*, 34(1), 21-36. <https://doi.org/10.1080/17445760.2017.1331438>.
- Kassogu , H., Bernoussi, A., Ma toug, M., & Amharref, M. (2017b). A two-scale cellular automaton for flow dynamics modeling (2CAFDYM). *Applied Mathematical Modelling*, 43, 61-77. <https://doi.org/10.1016/j.apm.2016.10.034>.
- Kim, H., Kim, J., Li, W., Yang, P., & Cao, Y. (2017). Exploring the impact of green space health on runoff reduction using NDVI. *Urban Forestry & Urban Greening*, 28, 81-87. <https://doi.org/10.1016/j.ufug.2017.10.010>.
- Knight, J. E. (2022). *Soil-Water-Balance (SWB) model archive used to simulate potential mean annual recharge in the Grand Canyon region, Arizona*. Reston: U.S. Geological Survey.

- Kuhn, M., & Johnson, K. (2013). *Applied predictive modeling* (p. 2). New York: Springer.
- Li, F., Zhang, G., Li, H., & Lu, W. (2019). Land Use Change Impacts on Hydrology in the Nenjiang River Basin, Northeast China. *Forests, 10*(6), 476.
<https://doi.org/10.3390/f10060476>.
- Liaqat, M., Mohamed, M., Chowdhury, R., Elmahdy, S., Khan, Q., & Ansari, R. (2021). *Impact of land use/land cover changes on groundwater resources in Al Ain region of the United Arab Emirates using remote sensing and GIS techniques*. *Groundwater For Sustainable Development, 14*, 100587.
<https://doi.org/10.1016/j.gsd.2021.100587>.
- Listings. RealtyAustin.com. (2022). Retrieved 26 July 2022, from
<https://www.realtyaustin.com/listings/neighborhood/tx/barton-creek/barton-creek?maxlat=30.338769269513424&minlong=-97.94629004566015&minlat=30.217653474224274&maxlong=-97.78630164233984&z=13>.
- Liu, X., Wei, M., & Zeng, J. (2020). Simulating Urban Growth Scenarios Based on Ecological Security Pattern: A Case Study in Quanzhou, China. *International Journal of Environmental Research and Public Health, 17*(19), 7282.
<https://doi.org/10.3390/ijerph17197282>.
- Lynch, K., & Rodwin, L. (1958). A Theory of Urban Form. *Journal of the American Institute of Planners, 24*(4), 201-214.
<https://doi.org/10.1080/01944365808978281>.

- Mahiny, A., & Gholamalifard, M. (2007). Dynamic Spatial Modeling of Urban Growth through Cellular Automata in a GIS Environment. *International Journal of Environmental Research*, 1(2), 272 - 279.
- Mahiny, A., & Clarke, K. (2012). Guiding SLEUTH land-use/land-cover change modeling using multicriteria evaluation: towards dynamic sustainable land-use planning. *Environment And Planning B: Planning and Design*, 39(5), 925-944. <https://doi.org/10.1068/b37092>.
- Mair, A., Hagedorn, B., Tillery, S., El-Kadi, A., Westenbroek, S., Ha, K., & Koh, G. (2013). Temporal and spatial variability of groundwater recharge on Jeju Island, Korea. *Journal Of Hydrology*, 501, 213-226. <https://doi.org/10.1016/j.jhydrol.2013.08.015>.
- McCoy, K. J., & Ladd, D. E. (2019). Documentation of a soil-water-balance model to estimate recharge to Blue Ridge, Piedmont, and Mesozoic basin fractured-rock aquifers, Fauquier County, Virginia, 1996 through 2015. *Scientific Investigations Report*. <https://doi.org/10.3133/sir20195056>.
- Mekonnen, Y., & Ghosh, S. (2020). Urban Growth and Land Use Simulation Using SLEUTH Model for Adama City, Ethiopia. *Advances Of Science and Technology*, 279 - 293. https://doi.org/10.1007/978-3-030-43690-2_19.
- Mensah, J., Ofosu, E., Yidana, S., Akpoti, K., & Kabo-bah, A. (2022). Integrated modeling of hydrological processes and groundwater recharge based on land use land cover, and climate changes: A systematic review. *Environmental Advances*, 8, 100224. <https://doi.org/10.1016/j.envadv.2022.100224>.

- Miles, L., Breitbart, S., Wagner, H., & Johnson, M. (2019). Urbanization Shapes the Ecology and Evolution of Plant-Arthropod Herbivore Interactions. *Frontiers In Ecology and Evolution*, 7. <https://doi.org/10.3389/fevo.2019.00310>.
- Mondal, K., Rathod, K., Joshi, H., Mandal, H., Khan, R., & Rajendra, K. et al. (2022). *Impact of Land-use and Land-cover Change on Groundwater Quality and Quantity in the Raipur, Chhattisgarh, India: A Remote Sensing and GIS approach*. In *Earth and Environmental Science* (p. 1). IOP Conference Series. Retrieved 24 July 2022.
- Musgrove, M., Opsahl, S., Mahler, B., Herrington, C., Sample, T., & Banta, J. (2016). *Source, variability, and transformation of nitrate in a regional karst aquifer: Edwards aquifer, central Texas*. *Science Of the Total Environment*, 568, 457-469. <https://doi.org/10.1016/j.scitotenv.2016.05.201>.
- Nardi, M. (2018). *Soil-Water Balance model datasets used to estimate groundwater recharge in Florida and parts of Georgia, Alabama, and South Carolina, 1895-2010*. Reston: U.S. Geological Survey.
- Neumann, J., & Burks, A. (1966). *Theory of self-reproducing automata. Edited and completed by Arthur W. Burks*. Illinois University Press.
- Nielson, M. (2019). *Soil-Water Balance model datasets used to estimate groundwater recharge in Florida and parts of Georgia, Alabama, and South Carolina, 1895-2010*. Reston: U.S. Geological Survey.
- Norton, W. (1978). Process and Form Relationships: And Example from Historical Geography. *The Professional Geographer*, 30(2), 128-134. <https://doi.org/10.1111/j.0033-0124.1978.00128.x>.

- Novak, S. (2021). *Austin's Stratus Properties plans 475 homes in final section of upscale Barton Creek project*. Statesman.com. Retrieved 26 July 2022, from <https://www.statesman.com/story/business/real-estate/2021/04/28/austins-stratus-properties-plans-475-homes-final-section-upscale-barton-creek-project/7391989002/>.
- Openshaw, S., (eds.) Abrahart, R., & See, L. (2014). *Geocomputation* (2nd ed., p. 3). CRC Press.
- Oregon State University. (2014, February 4). PRISM Climate Group. Retrieved October 24, 2022, from <https://prism.oregonstate.edu/>.
- Park, E., Jeong, J., Choung, S., Han, W., Kim, K., & Suk, H. (2021). A Method for Integrating Delayed Recharge Flux Through Unsaturated Zones into Analytical and Numerical Groundwater Flow Modeling. *Water Resources Research*, 57(3). <https://doi.org/10.1029/2020wr027655>.
- Prabhakar, A., & Tiwari, H. (2015). *Land use and land cover effect on groundwater storage*. *Modeling Earth Systems and Environment*, 1(4). <https://doi.org/10.1007/s40808-015-0053-y>.
- Rafiee, R., Mahiny, A., Khorasani, N., Darvishsefat, A., & Danekar, A. (2009). Simulating urban growth in Mashad City, Iran through the SLEUTH model (UGM). *Cities*, 26(1), 19-26. <https://doi.org/10.1016/j.cities.2008.11.005>.

- Raven, J., Stone, B., Mills, G., Towers, J., Katzschner, L., Leone, M., Gaborit, P., Georgescu, M., and Hariri, M. (2018). Urban planning and design. In Rosenzweig, C., W. Solecki, P. Romero-Lankao, S. Mehrotra, S. Dhakal, and S. Ali Ibrahim (eds.), *Climate Change and Cities: Second Assessment Report of the Urban Climate Change Research Network*. Cambridge University Press. New York. 139–172.
- Rienow, A., & Goetzke, R. (2015). Supporting SLEUTH – Enhancing a cellular automaton with support vector machines for urban growth modeling. *Computers, Environment And Urban Systems*, 49, 66-81.
<https://doi.org/10.1016/j.compenvurbsys.2014.05.001>.
- Rorabaugh, M. I., & Simons, W. D. (1966). Exploration of methods of relating ground water to surface water, Columbia River basin-second phase. *Open-File Report*.
<https://doi.org/10.3133/ofr66117>.
- Sakieh, Y., Amiri, B., Danekar, A., Feghhi, J., & Dezhkam, S. (2014a). Scenario-based evaluation of urban development sustainability: an integrative modeling approach to compromise between urbanization suitability index and landscape pattern. *Environment, Development And Sustainability*, 17(6), 1343-1365.
<https://doi.org/10.1007/s10668-014-9609-7>.
- Sakieh, Y., Amiri, B., Danekar, A., Feghhi, J., & Dezhkam, S. (2014b). Simulating urban expansion and scenario prediction using a cellular automata urban growth model, SLEUTH, through a case study of Karaj City, Iran. *Journal Of Housing and The Built Environment*, 30(4), 591-611. <https://doi.org/10.1007/s10901-014-9432-3>.

- Sakieh, Y., Salmanmahiny, A., Jafarnezhad, J., Mehri, A., Kamyab, H., & Galdavi, S. (2015). Evaluating the strategy of decentralized urban land-use planning in a developing region. *Land Use Policy*, 48, 534-551.
<https://doi.org/10.1016/j.landusepol.2015.07.004>.
- Sakieh, Y., & Salmanmahiny, A. (2016). Treating a cancerous landscape: Implications from medical sciences for urban and landscape planning in a developing region. *Habitat International*, 55, 180-191.
<https://doi.org/10.1016/j.habitatint.2016.03.008>.
- Shi, G., Lu, X., Zhang, H., Zheng, H., Zhang, Z., & Chen, S. et al. (2022). *Air pollutant emissions induced by rural-to-urban migration during China's urbanization (2005–2015)*. *Environmental Science and Ecotechnology*, 10, 100166.
<https://doi.org/10.1016/j.es.2022.100166>.
- Shuler, C., Brewington, L., & El-Kadi, A. (2021). A participatory approach to assessing groundwater recharge under future climate and land-cover scenarios, Tutuila, American Samoa. *Journal Of Hydrology: Regional Studies*, 34, 100785.
<https://doi.org/10.1016/j.ejrh.2021.100785>.
- Silva, E., & Clarke, K. (2002). Calibration of the SLEUTH urban growth model for Lisbon and Porto, Portugal. *Computers, Environment and Urban Systems*, 26(6), 525-552. [https://doi.org/10.1016/s0198-9715\(01\)00014-x](https://doi.org/10.1016/s0198-9715(01)00014-x)
- Smith, M., Winkler, R., & Johnson, K. (2016). *How Migration Impacts Rural America*. Michigan Technological University. Retrieved from https://w3001.apl.wisc.edu/b03_16.

- Sonoda, K., Yeakley, J., & Walker, C. (2001). *Near-stream land use effects on stream water nutrient distribution in an urbanizing watershed*. *Journal Of the American Water Resources Association*, 37(6), 1517-1532.
<https://doi.org/10.1111/j.1752-1688.2001.tb03657.x>.
- Sunde, M., He, H., Hubbart, J., & Scroggins, C. (2016). Forecasting streamflow response to increased imperviousness in an urbanizing Midwestern watershed using a coupled modeling approach. *Applied Geography*, 72, 14-25.
<https://doi.org/10.1016/j.apgeog.2016.05.002>.
- Sung, C., Yi, Y., & Li, M. (2013). Impervious surface regulation and urban sprawl as its unintended consequence. *Land Use Policy*, 32, 317-323. <https://doi.org/10.1016/j.landusepol.2012.10.001>.
- Texas A&M University. (2020). *Texas will face driest conditions of the last 1,000 years*. ScienceDaily. Retrieved from <http://www.sciencedaily.com/releases/2020/07/200708121419.htm>.
- Texas Politics Project. (2022). *THE TRANSFORMATION OF THE TEXAS ECONOMY*. Austin: University of Texas at Austin. Retrieved from <https://texaspolitics.utexas.edu/educational-resources/transformation-texas-economy>.
- Texas State Library. (2020). *United States and Texas Populations 1850-2017*. Austin: Texas State Library and Archives Commission. Retrieved from <https://www.tsl.texas.gov/ref/abouttx/census.html>.
- Tobler, W. (1979). In: *Gale, S., Olsson, G. (eds) Philosophy in Geography. Theory and Decision Library, vol 20*. Dordrecht: Springer.

- Torrey, B. (2004). *Urbanization: An Environmental Force to Be Reckoned With*. Washington: Population Reference Bureau. Retrieved from <https://www.prb.org/resources/urbanization-an-environmental-force-to-be-reckoned-with/>.
- U. S. Census Bureau. (2017). *One in Five Americans Live in Rural Areas*. Census.gov. Retrieved from <https://www.census.gov/library/stories/2017/08/rural-america.html>.
- U. S. Census Bureau. (2022). *Over Two-Thirds of the Nation's Counties Had Natural Decrease in 2021*; Release number CB22-51. Census.gov. Retrieved from <https://www.census.gov/newsroom/press-releases/2022/population-estimates-counties-decrease.html#:~:text=MARCH%2024%2C%202022%20%E2%80%94%20More%20than,components%20of%20change%20released%20today>.
- U. S. Geological Survey. (2021a). *New Groundwater Model Provides Better Understanding of Edwards Aquifer*. USGS.gov. Retrieved from <https://www.usgs.gov/news/new-groundwater-model-provides-better-understanding-edwards-aquifer>.
- U. S. Geological Survey. (2021b). *What is a fault and what are the different types?*. USGS.gov. Retrieved from https://www.usgs.gov/faqs/what-a-fault-and-what-are-different-types?qt-news_science_products=0#qt-news_science_products.

- Wang, R., Bai, Y., Alatalo, J., Yang, Z., Yang, Z., Yang, W., & Guo, G. (2021a). *Impacts of rapid urbanization on ecosystem services under different scenarios – A case study in Dianchi Lake Basin, China*. *Ecological Indicators*, 130, 108102. <https://doi.org/10.1016/j.ecolind.2021.108102>.
- Wang, K., Onodera, S., Saito, M., & Shimizu, Y. (2021b). Long-term variations in water balance by increase in percent imperviousness of urban regions. *Journal Of Hydrology*, 602, 126767. <https://doi.org/10.1016/j.jhydrol.2021.126767>.
- Watershed Protection Department. (2016a). *Master Plan* (pp. 200-201). Austin: City of Austin.
- Watershed Protection Department. (2016b). *Master Plan* (pp. 288). Austin: City of Austin.
- Westenbroek, S., Nielson, M., & Ladd, D. (2021). *OFR 2021-1008 MODEL ARCHIVE: Soil-Water-Balance model developed to simulate net infiltration and irrigation water use for the Mississippi Embayment Regional Aquifer System, 1915 to 2018*. Reston: U.S. Geological Survey.
- Westenbroek, S., Kelson, V., Dripps, W., Hunt, R., & Bradbury, K. (2010). *A Modified Thornthwaite-Mather Soil-Water-Balance code for estimating groundwater recharge*. U. S. Geological Survey.
- White, S., Potter, L., You, H., Valencia, L., Jordan, J., Pecotte, B., & Robinson, S. (2017). *Urban Texas* (p. 1). San Antonio: Texas Demographic Center. Retrieved from https://demographics.texas.gov/Resources/publications/2017/2017_08_21_UrbanTexas.pdf.

- Wilson, A. (1977). *Spatial interaction and settlement structure: toward an explicit Central Place Theory* (pp. 137 - 156). Leeds: University of Leeds.
- Wolfram, S. (1994). *Cellular Automata and Complexity: Collected Papers by Stephen Wolfram* (1st ed.). CRC Press.
- Wright, M., Santelmann, M., Vaché, K., & Hulse, D. (2021). Modeling the impact of development policies and climate on suburban watershed hydrology near Portland, Oregon. *Landscape And Urban Planning*, 214, 104133. <https://doi.org/10.1016/j.landurbplan.2021.104133>.
- Wu, J., Xiang, W., & Zhao, J. (2014). *Urban ecology in China: Historical developments and future directions*. *Landscape And Urban Planning*, 125, 222-233. <https://doi.org/10.1016/j.landurbplan.2014.02.010>.
- Wu, P., Shu, L., Comte, J., Zuo, Q., Wang, M., Li, F., & Chen, H. (2021). The effect of typical geological heterogeneities on the performance of managed aquifer recharge: physical experiments and numerical simulations. *Hydrogeology Journal*, 29(6), 2107-2125. <https://doi.org/10.1007/s10040-021-02375-3>.
- Xiang, W., & Clarke, K. (2003). The Use of Scenarios in Land-Use Planning. *Environment and Planning B: Planning and Design*, 30(6), 885-909. <https://doi.org/10.1068/b2945>.
- Yang, X., & Lo, C. (2003). Modelling urban growth and landscape changes in the Atlanta metropolitan area. *International Journal Of Geographical Information Science*, 17(5), 463-488. <https://doi.org/10.1080/1365881031000086965>.

- Yao, F., Zhu, H., & Wang, M. (2021). *The Impact of Multiple Dimensions of Urbanization on CO2 Emissions: A Spatial and Threshold Analysis of Panel Data on China's Prefecture-Level Cities*. *Sustainable Cities and Society*, 73, 103113. <https://doi.org/10.1016/j.scs.2021.103113>.
- Yar, P. (2020). *Urban development and its impact on the depletion of groundwater aquifers in Mardan City, Pakistan*. *Groundwater For Sustainable Development*, 11, 100426. <https://doi.org/10.1016/j.gsd.2020.100426>.
- Zappitello, S., Johns, D., & Hunt, B. (2019). *Summary of Groundwater Tracing in the Barton Springs Edwards Aquifer from 1996 to 2017*. Austin: City of Austin Watershed Protection. Retrieved from <https://bseacd.org/uploads/Zappitello-et-al.-2019-Dye-Tracing-Summary.pdf>.
- Zhang, Y., & Schilling, K. (2006). *Effects of land cover on water table, soil moisture, evapotranspiration, and groundwater recharge: A Field observation and analysis*. *Journal Of Hydrology*, 319(1-4), 328-338. <https://doi.org/10.1016/j.jhydrol.2005.06.044>.
- Zhao, C., Weng, Q., & Hersperger, A. (2020). Characterizing the 3-D urban morphology transformation to understand urban-form dynamics: A case study of Austin, Texas, USA. *Landscape And Urban Planning*, 203, 103881. <https://doi.org/10.1016/j.landurbplan.2020.103881>.
- Zhu, C., Zhang, X., Zhou, M., He, S., Gan, M., Yang, L., & Wang, K. (2020). *Impacts of urbanization and landscape pattern on habitat quality using OLS and GWR models in Hangzhou, China*. *Ecological Indicators*, 117, 106654. <https://doi.org/10.1016/j.ecolind.2020.106654>.